Review on Recent Progress and Reactor Set-Ups for Hydrogen Production from Formic Acid Decomposition

Sanaa Hafeez[1#*], Eleana Harkou[2#], Anastasia Spanou[2], Sultan Al-Salem[3], Alberto Villa[4], Nikolaos Dimitratos[5], George Manos[1] and Achilleas Constantinou[2*].

1. Department of Chemical Engineering, University College London, London WCIE 7JE, UK.
2. Department of Chemical Engineering Cyprus University of Technology, 57 Corner of Athinon and Anexartisias, 3036 Limassol, Cyprus.
3. Environment & Life Sciences Research Centre, Kuwait Institute for Scientific Research, P.O. Box: 24885, Safat 13109, Kuwait.
4. Dipartimento di Chimica, Universitá degli Studi di Milano, via Golgi, 20133 Milan, Italy.
5. Dipartimento di Chimica Industriale e dei Materiali, ALMA MATER STUDIORUM Università di Bologna, Viale Risorgimento 4, 40136 Bologna, Italy.

* Authors for correspondence: a.konstantinou@cut.ac.cy; sanaa.hafeez@ucl.ac.uk

\# These authors share first authorship

Abstract

Hydrogen is a clean and efficient energy carrier, and a hydrogen-based economy is an alternative solution for the sustainability. The present work reviews the recent progress for hydrogen's production from various technologies including the generation from fossil fuels, from biomass through biological and thermochemical processes and from water splitting. Although hydrogen is a zero-emission energy when it is used, its cleanness depends on the production pathway that preceded. Hydrogen's storage and transportation has been costly and an unsafe procedure, formic acid, on the other hand, can be generated, transported, and decomposed easily to hydrogen. Formic acid is generated from the hydrogenation of atmospheric CO_2 and can easily provide with energy portable devices, vehicles, and other applications. In addition, the most widely known homogeneous and heterogeneous catalysts and reactors for the formic acid reaction are presented. Different types of reactors like, fixed-bed reactors, batch reactors, CSTR and microreactors were assessed for their performance and reaction's efficiency during formic acids decomposition.

Keywords: Formic Acid, Dehydrogenation, Reactors, Hydrogen, Membrane, Sustainable.

1. Introduction

Energy demands increase every year with the combustion of conventional fossil fuels creating serious global climate and environmental issues and their early depletion [1]. The need for alternative environmentally friendly energy sources has become a serious topic in recent years. With hydrogen being a clean energy carrier with zero emissions, much research has emerged to study its potential and develop new ways of utilising it. One of the most beneficial ways of utilising hydrogen, not just from an economic standpoint, but also as a possible solution to the escalating problem that greenhouse gas emissions are causing, is replacing the fossil fuel dependency with hydrogen.

Hydrogen offers a promising alternative to conventional fuels because it can be generated by the electrolysis of water and effectively transformed on-demand into electricity by fuel cells [2-6]. Nevertheless, feasible options in the delivery and storage of hydrogen have not achieved a practical level because of the safety issues and the big energy loss in the hydrogen liquefaction step and boil-off during transportation [7, 8]. Fuel cells have great developing potential and may play a significant role in power generation in the future. There are numerous applications in several areas ranging from public transportation vehicles to submarines and spacecrafts, from portable devices to stationary power generators and more [9].

Formic acid (FA), as a hydrogen carrier, is a promising route to the production of hydrogen due to the fact that it's decomposition can take place at mild conditions, and it is safer during transportation [1, 10-14]. The application of formic acid as a secondary fuel has been investigated through the use of direct formic acid fuel cells (DFAFCs) [15-20]. On the other hand, the decomposition of formic acid to generate hydrogen for polymer electrolyte membrane fuel cells (PEMFCs) is a promising alternative as a mature technology [21, 22].

Williams et al. [23] were the first whom suggested the CO_2 reduction to FA that can be converted to hydrogen in the late 1970s. There are two pathways of FA decomposition, with the first one to include the decarboxylation toward CO_2 and H_2, and the other one, the decarbonylation toward CO and H_2O which should be inhibited, the chemical reactions are shown below respectively [24].

$$HCOOH(l) \rightarrow CO_2 + H_2 \tag{1}$$

$$HCOOH(l) \rightarrow CO + H_2O \tag{2}$$

The formation of CO should be avoided due to poisoning of the catalysts. A lot of investigations were made on the catalytical decomposition of FA and the high selectivity of H_2. Bulushev et al. [25], used Pd and Au catalysts for the reaction where it took place in the vapour phase. They showed that the water-gas shift reaction was more favorable after the addition of water vapour where it improved the selectivity of the catalyst. Whilst, Hu et al. [26], studied the reaction mechanisms for gas and aqueous phase decomposition of FA to rich gas H_2 using several noble metals. Homogeneous and heterogeneous catalysts may be used with the first one can leach out and has problems with water content. From the other point of view, heterogeneous catalysts can be shaped into a bed of any geometry solving these problems [27].

As previously mentioned, the generation of FA can be made via the catalytic hydrogenation CO_2, or bicarbonate, with suitable catalysts. The levels of CO_2 in the atmosphere are increasing annually, causing global environmental crisis, since the CO_2 is one of the major greenhouse gases. The hydrogenation of CO_2 gives great potential to minimise those emissions [28]. The hydrogenation of CO_2 is exothermic and strongly endergonic reaction, in contrast to when base (ammonia) is present in the process which an exothermic protonation of the base by FA delivers energy to make the reaction exergonic [29]. The direct hydrogenation of CO_2 is usually taking place in aqueous solutions in the presence of ammonia is described by Eq. 3 [28].

$$CO_{2\,(aq)} + H_{2\,(aq)} + NH_{3\,(aq)} \rightarrow HCOO^-{}_{(aq)} + NH_4^+{}_{(aq)} \tag{3}$$
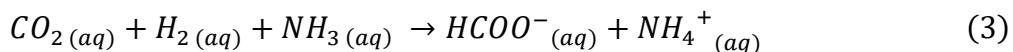
In this review, the hydrogen storage challenges, and various hydrogen production routes (conventional and renewable) will be discussed. This will be followed by the catalysts used for FA decomposition, homogeneous and heterogeneous, and the structural and physiochemical properties of the catalysts will bepresented showing selected examples. A number of reviews have covered the decomposition of formic acid, focusing on the types of catalysts applied and the formic acid production routes and focusing on structure-function relationships [1, 12, 30-33]. Therefore, the current review focuses on and offers insights into the reactor types and set-ups which have been applied for the FA decomposition process and highlights the most efficient and novel systems.

## 2. Hydrogen storage challenges

One of the main challenges and restrictions for the utilisation of hydrogen is facing, is the difficulty in its storage and transportation as these factors can have a crucial impact on the final cost of hydrogen. These challenges transpire from hydrogen's extremely low density of 0.08376 kg/m^3 (at 20 °C and 1 atm) which means that 1 kg of H$_2$ requires 11.9 m^3 and also the wide range of concentrations of H$_2$ in the air (at atmospheric conditions) at which hydrogen is flammable and explosive [34].

Therefore, in order for hydrogen to become a viable option as an energy carrier, it needs to be stored in higher densities since, in its natural form a lot of volume is required for small amounts of energy. While research interest on hydrogen storage focuses on the efficiency and affordability regarding capital and operating costs along with their energy requirements, the environmental impact and safety should not be neglected. Further standards and regulations should be implemented to ensure safety by eliminating the possibility of any accidents and negative impacts on the environment and human health as much as possible [35]. An extremely attractive and perhaps the most suitable storage solution that is already being used is the injection of hydrogen in salt caverns. This method offers great advantages such as low construction cost, fast injection, and withdrawal rates as well as low leakage rates, cushion gas requirements and contamination risks. Unfortunately, this method is not always an option as certain regions do not require the necessary geological characteristics to host a salt cavity storage [36].

In consequence, the development of other efficient storage solutions is still necessary. I.A. Hassan et al. [35] state that supercapacitors are the best option for peak loads of hydrogen were as hydrogen storage systems (HSSs) and battery energy storage systems (BESS) are applicable for long and short term storage respectively. Hydrogen storage systems (HSSs) are separated into physical storage (PS) and material based (chemical) storage. PS methods consist of compressed gas hydrogen storage (CGH$_2$), Liquid hydrogen storage (LH$_2$) and cryo-compressed hydrogen storage were hydrogen, in its pure form, is compressed, cooled or both accordingly, by altering the temperature and pressure of storing conditions. Material based storage is divided into adsorption or absorption techniques with the later focusing on either metal hydrides or chemical hydrides.

Among the previously mentioned technologies, chemical hydrogen storage in chemical hydrides, which store hydrogen with chemical bonds inside their molecules, in either solid or liquid phase

materials, holds several advantages. To begin with chemical storage in general it is a much safer alternative to physical hydrogen storage as it does not require extreme conditions (low T, high P) [37]. Solid state materials demonstrate several drawbacks such as their slow kinetics for hydrogen release and deterioration of the solid material after consecutive cycles, as well as heat dissipation issues and the high temperatures hydrogen requires to desorb. Therefore, liquid phase materials with their high hydrogen density, safe storability and relative stability appear as a much more favourable alternative. These materials need to have the ability to release hydrogen from their molecules under mild conditions and some promising compounds that have received much attention are some boron-based compounds ($NaBH_2$, NH_3BH_3, $N_2H_4BH_3$), hydrous hydrazine and FA [37]. Fig. 1 shows the catalytic cycle for hydrogen storage in FA.
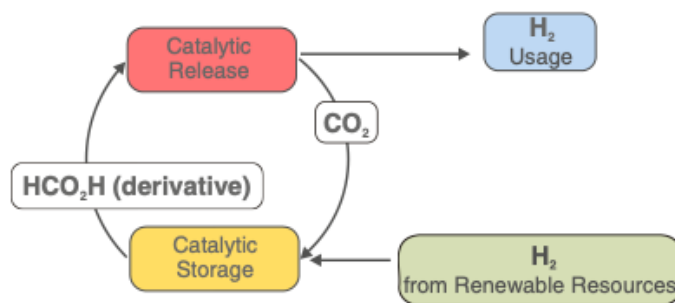
Figure 1. A catalytic cycle for hydrogen storage in FA [14].

3. Hydrogen production routes

Different types of hydrogen production methods have been in development for the past two decades with many of them already being used for large scale production. These methods can be separated into two main categories distinguished based on their feedstock which can either come from fossil fuels or renewable sources.

3.1 Conventional production methods

Steam reforming (SR) is currently considered the most developed and economically efficient method for hydrogen production, not just among the reforming techniques but also most commercial techniques. The feedstock can vary from natural gas and liquified petroleum gas (LPG), to naphtha and kerosene. The metal-based catalysts (mostly nickel) used in reforming processes need a sulphur-free feedstock to cut back on catalyst deactivation and therefore a

desulphurisation unit is required [38, 39]. Then the process begins with the reformer unit, a tubular catalytic reactor, where the hydrocarbon feed is mixed with steam producing syngas (mainly H_2 and CO with low amounts of CO_2). The reaction is endothermic and requires elevated temperatures and pressures up to 800-900 °C and 3.5 MPa.

Currently, steam methane reforming (SMR) is the most commonly used industrial method for hydrogen production but studies have shown that steam reforming of natural gas (SRNG) is the most economically viable method with the lowest H_2/CO_2 ratio out of all hydrocarbons [40, 41]. Steam reforming is more desirable than partial oxidation (POX) and autothermal reforming (ATR) reforming methods. Its endothermic nature allows the reactions to be carried out with lower temperatures and the higher H/CO ratio it provides which is the ultimate goal [38].

Another way to achieve hydrogen's production is through the pyrolysis pathway. Pyrolysis is presently proving to be a highly promising method for hydrogen production with slow and fast pyrolysis being the two types most frequently used for this purpose [40]. The process comprises of the dehydration of the hydrocarbons and then thermal decomposition (gasification) under extreme heat that ranges at 500-900 °C in the absence of oxygen and air. Therefore, the process following Eq. 4:

$$C_nH_m + heat \rightarrow nC_{(s)} + 0.5mH_2 \tag{4}$$
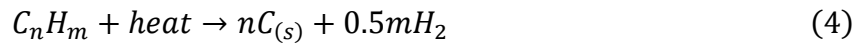
does not produce any carbon oxides (CO_2 and CO) offering substantial emissions reduction. However, any residues of air or water from inadequate drying of the materials can result in significant CO_x emissions. Among the simplicity and compactness of this method, another important advantage is the fuel flexibility, which can vary from hydrocarbons to any type of organic material and waste that could potentially facilitate waste disposal.

Although many scientists have been devoted to steam reforming of pure glycerol, Dang et al. [42] were investigated the effect of common impurities in crude glycerol on the H_2 production. The steam reforming of glycerol was held under the presence of Ni-based catalyst and was obtained that the presence of methanol increased the H_2 yield while acetic acid and oleic acid decreased H_2 yield and hydrocarbons conversion and enhanced the formation of coke. Sahraei et al. [43] investigated the effects of catalysts synthesis parameters and operating temperature on the properties and catalytic performance of Ni-promoted Fe_2O_3 and MgO oxide metal catalysts for H_2 production by glycerol steam reforming. At optimum operating conditions and 5 wt.% Ni

incorporated onto the catalysts higher H_2 yield, and very low coke formation obtained resulting the almost complete conversion of glycerol. At higher temperatures it was observed that suppress coke was formed limiting the Boudouard reaction, with a drawback of lower H_2 yield.

Charisiou et al. [44] investigated the activity and the impact of the addition of La and Ce metal oxides into a Ni-based catalyst for the dry reforming of biogas. The study not only focuses on the characteristic of fresh and spent catalysts but also on the amount and type of coke deposition. It was concluded that both catalysts had promoting effects such as enhanced catalytic activity and stability. Also, the amount of deposited coke was decreased linearly with temperature with a higher slope on the modified samples due to the faster oxidation on the catalysts at higher temperatures.

The dry reforming of bio-gas derived from anaerobic digestion of biomass was examined by Hajizadeh et al. [45]. A kinetic model was developed incorporating both processes (anaerobic digestion and dry reforming) with the observed results having a good agreement with experimental ones. Many effects have been studied in order to design an optimum operating system with highest conversion of CH_4 to H_2 and lowest energy consumption. The overall conversion (biomass to H_2) showed an energetic efficiency of 72.85% revealing its superiority to similar processes, such as steam and auto-thermal reforming. Also, this process highlights a high potential for atmospheric CO_2 reduction.

Yoo et al. [46] studied the ethanol steam reforming using a series of K-promoting cobalt catalysts. The promotion effect of K showed an enhancing performance on H_2 yield and an obstruction of the undesired methanation reaction. However, the excess amount of K doping blocked small pores of the support of the catalyst, resulting in deterioration of the textural property of the catalyst. Ni- and Co-based materials were found to have an enhanced activity on bio-oil steam reforming in comparison with other transition metal-based catalysts. Bio-oil contains a range of oxygenated organic compounds which promote the formation of coke [47]. Megía et al. [48] investigated the deactivation of a Co/SBA-15 catalyst during the steam reforming of the aqueous fraction of bio-oil and observed that cause of deactivation of the catalyst is due to the amount of coke deposited and the C/H ratio of hydrocarbons.
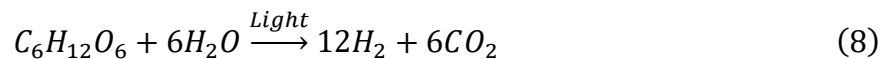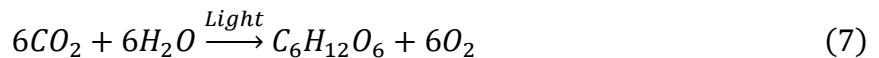
3.2 Renewable production methods

3.2.1 Biomass to hydrogen

Biorefinery systems have started gaining a lot of attention lately due to the low operational cost and sustainable and environmentally friendly processes. Energy supply by hydrogen production could be one of their future purposes if further research manages to overcome the main limitations of biological conversion routes such as their low hydrogen production rate and yield [49]. The main groups of biomass feedstock used for this purpose are pure carbohydrates, food-substrate and wastewater sludge usually derived from industrial waste and the main biological conversion pathways are bio photolysis and fermentation with the most available resource currently being lignocellulosic biomass [50, 51]. The dominant microorganisms that involve in the biohydrogen production are, *Clostridium spp., Enterobacter spp., Bacillus spp., E. coli, Klebsiella spp.* and thermophilic lactic acid bacteria [52].

The method of bio-photolysis uses the same processes of photosynthesis found at plants and algal but utilise them for H_2 production [53]. Bio-photolysis can be either direct or indirect with the first one to promote the direct conversion of water molecules to hydrogen under anaerobic conditions, by photoautotrophic organisms with the enzymatic catalytic activity of hydrogenase, with the reactions to be [54]:

$$H_2O \xrightarrow{Light} \frac{1}{2}O_2 + 2H^+ + 2e^- \tag{5}$$

$$2H^+ + 2e^- \xrightarrow{Hydrogenase} H_2 \tag{6}$$
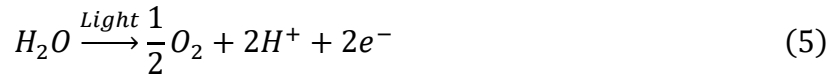
Indirect bio-photolysis is carried out by the combination of two biological processes, photosynthesis and fermentation, also involving hydrogenase under anaerobic conditions. This process includes the fixation of environmental CO_2 to carbohydrates by photosynthesis in the presence of light which are then converted into hydrogen by fermentation with the help of hydrogenase with or without light [49]. The indirect photolysis is presented as follow [54]:

$$6CO_2 + 6H_2O \xrightarrow{Light} C_6H_{12}O_6 + 6O_2 \tag{7}$$

$$C_6H_{12}O_6 + 6H_2O \xrightarrow{Light} 12H_2 + 6CO_2 \tag{8}$$

Fermentation is another process that can lead to the high production of bio-hydrogen using microorganisms without the generation of O_2. There are two distinct types depending on the presence of light, dark and photo fermentation. Dark-fermentation or anaerobic fermentation is caried out in darkness with anaerobic conditions and produces hydrogen by anaerobic digestion/decomposition of organic carbon substrates by anaerobic bacteria such as *Enterobacter, Bacillus, Clostridium, and Escherichia coli* [55]. Acetic and butyric acids are the most common products of dark-fermentation while H_2 is a by-product of the process, with the reactions as follows [56]:

$$C_6H_{12}O_6 + 2H_2O \rightarrow 2CH_3COOH + 2CO_2 + 4H_2 \tag{9}$$

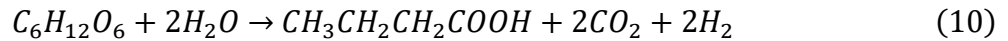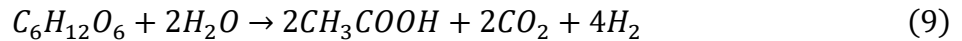$$C_6H_{12}O_6 + 2H_2O \rightarrow CH_3CH_2CH_2COOH + 2CO_2 + 2H_2 \tag{10}$$

Photo-fermentation is performed in aerobic or anaerobic conditions, by many photosynthetic bacteria that utilise light as an energy source to convert organic compounds into hydrogen and CO_2. It is an environmentally friendly process with the capability to generate H_2 at large-scale at no extreme temperature and pressure [57]. The reaction which describes the process is:

$$C_6H_{12}O_6 \xrightarrow{Light} 6CO_2 + 12H_2 \tag{11}$$

Gasification and Pyrolysis are the dominating thermochemical processing methods for biomass as they have shown the most promising results and potential [58-61]. These two processes include the conversion of biomass to syngas and bio-oils and therefore the hydrogen production via the water gas shift (WGS) reaction and the autothermal reforming of bio-oils, respectively [62]. Fig. 2 shows these two thermochemical H_2 production processes from biomass feedstock. On the other hand liquification and combustion have limited potential, with liquification emitting polluting by-products and gasification requiring very high pressures up to 20 MPa which are hard to achieve and along with the methods' low efficiency on H_2 production hence, making them less favorable [41].
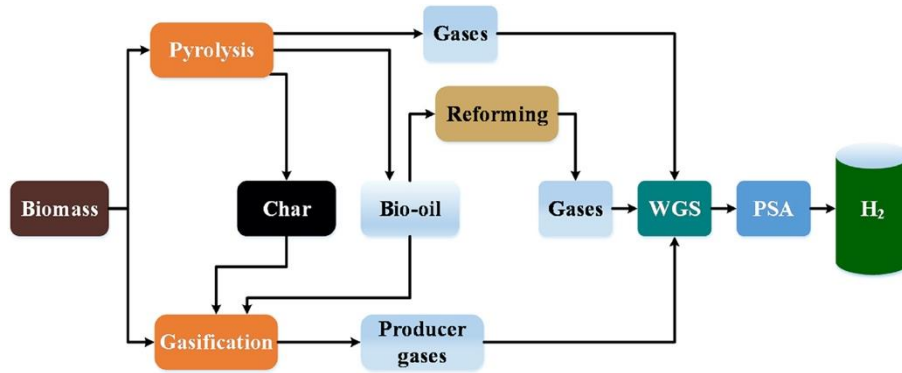
Figure 2. Hydrogen production by thermochemical conversion of biomass [61].

Biomass gasification is the most prominent route compared to the other three thermochemical processes due to the fact that it produces clean products, has lower pollutant emissions and is more efficient [63]. The biomass gasification is an endothermic process that requires an oxidising/gasifying agent to produce CO, H_2, CO_2, light hydrocarbons, tar, char and water at temperatures over 700 °C [62, 64]. The gasifying agent can either be air, oxygen or steam as shown in equation 2, therefore both the process and conditions change accordingly.

$$Biomass + steam \rightarrow H_2 + CO_2 + CO + CH_4 + HC + H_2O + Tar + Char \qquad (12)$$
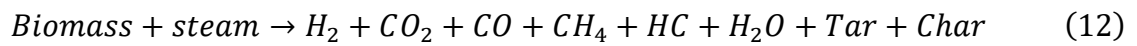
Steam gasification is the most promising method since it eliminates the difficulties of using air or oxygen, which includes the cost of removing hydrogen in the first and the high cost of oxygen for the later. In addition, steam gasification can be carried out with wet biomass, it has minimal impurities and produces a higher purity oxygen and H_2/CO ratio than the others [60].

Pyrolysis is another thermochemical method for converting biomass to H_2 greatly like gasification but can be caried out without an oxidising agent and in lower temperatures (400-800 °C) with up to 5 bar pressure. This process leads to the change of chemical composition and natural state of the organic material. The pyrolysis produces gaseous products like CO and H_2 (syngas), CO_2 and short hydrocarbon chain gases, liquid products known as bio-oils and tars. Pyrolysis is classified into three classes, depending on time and temperature of process: conventional (<400 °C), fast (450-600 °C) and flash (>600 °C) pyrolysis. The general reaction appears as follows [60] [36]:

$$Biomass + heat \rightarrow H_2 + CO + CO_2 + CH_4 + H_2O + bio - oil + char \qquad (13)$$

Nickel-based catalysts have been investigated widely by many scientists indicating the elimination of need for power and therefore the cost, and also that at high temperatures the catalysts are

deactivated by the deposition of coke [65, 66]. An advantage to this route, is the ability to optimise the temperature of each process individually as the two steps are carried out separately which helps minimising the catalyst deactivation. Even though this method focuses mainly on syngas production, the quality and concentration of the gasifying agent can be alternated to enhance H_2 production [58].
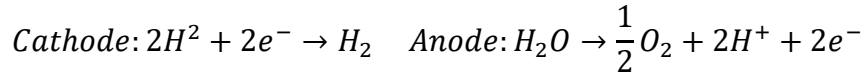
Cho et al. [67] studied the effect of the addition of CO_2 in the catalytic pyrolysis of a waste biomass in the presence of Ni-based catalyst. The presence of CO_2/N_2 promoted the conversion of biomass and the generation of syngas but also, enhanced the coke formation on the catalyst. The effect of preparation method of Fe-Co-K catalysts on biomass pyrolysis was investigated by Dai et al. [68]. The bimetallic materials showed better catalytic activity than the monometallic Fe-based. The co-precipitation method was beneficial for H_2 and CO yields due to the small crystallite size of the catalyst and the high crystallinity of the alloy.

The production of high-quality bio-oil with minimal water content and high HHV from forest residues biomass was studied by Chireshe et al. [69]. In the study, two oxide catalysts CaO and MgO, were used and both of them showed significant deoxygenation capabilities as the organic-rich phase HHV increased by 20 %. Concluding, the organic-rich phase of the first catalyst contained low water content at 7.8 wt.% and also CaO, enhanced the water-gas-shift reaction to H_2 production. Ma et al. [70] investigated the catalytic pyrolysis of algae biomass under different temperatures and under three type of zeolite catalysts. A maximum bio-oil of 41.3 wt.% was obtained in the presence of Y-zeolite. All the three catalysts showed high gas yield that might be attributed to a second cracking might occurred on the pyrolytic volatiles and promoted the larger small molecules.

3.2.2   Water to hydrogen

The three main technologies that are currently under development and will be analysed further are electrolysis that uses electricity, photo electrolysis that uses solar energy and finally thermochemical water splitting that requires heat. Electrolysis is an extensively studied and well-known method and has become highly desirable due to proving to be the most effective hydrogen-producing technique via water splitting [41]. In simple water electrolysis, water is the only reactant

that decomposes into H$_2$ and O$_2$ produced at the cell's anode and cathode respectively after electricity is provided to the cell as an energy source for the following endothermic reaction [71]:

$$Cathode: 2H^2 + 2e^- \rightarrow H_2 \quad Anode: H_2O \rightarrow \frac{1}{2}O_2 + 2H^+ + 2e^-$$

$$Overall: H_2O \rightarrow H_2 + \frac{1}{2}O_2 \qquad\qquad (14-16)$$

Water electrolysis is expected to become the method derived from renewable sources that will eventually facilitate the scale up of hydrogen production with zero emissions. This estimation is supported by the significant advantages of this method such as the high cell efficiency and high hydrogen production rate with purity that reaches 99.999% and pure oxygen as the only by-product and the abundant source of water [71, 72]. Currently the biggest obstacle, holding back the prevalence of electrolysis is the high electricity consumption of electrolysers. Electricity cost is the main expense of this method, but studies have shown that by using renewable energy sources (nuclear, solar, wind, geothermal) can become notably more cost effective and sustainable. This way not only H$_2$ from electrolysis becomes the cleanest energy carrier but the overall cost can compete with other large scale technologies [41, 72].

Since some renewable energy sources are not always available, they have unstable energy production. Therefore, efforts have been focused into the development and optimisation of the operating conditions, electrolyte, and ionic agents of different type of water electrolysis. There are four kinds of water electrolysis methods: i) Proton exchange membrane (PEM) water electrolysis, ii) Microbial electrolysis cells (MEC), iii) Alkaline water electrolysis (AWE), iv) Solid oxide electrolysis (SOE) as shown in Fig. 3 [72].

PEM Electrolysis

Anode: $H_2O \rightarrow 2H^+ + \frac{1}{2}O_2 + 2e^-$

Cathode: $2H^+ + 2e^- \rightarrow H_2$

Overall cell: $2H_2O \rightarrow H_2 + \frac{1}{2}O_2$

Alkaline Electrolysis

Anode: $2OH^- \rightarrow H_2O + \frac{1}{2}O_2 + 2e^-$

Cathode: $2H_2O + 2e^- \rightarrow H_2 + 2OH^-$

Overall cell: $H_2O \rightarrow H_2 + \frac{1}{2}O_2$

Microbial Electrolysis

Anode: $CH_3COO^- + 4H_2O \rightarrow 2HCO_3^- + 9H^+ + 8e^-$

Cathode: $8H^+ + 8e^- \rightarrow 4H_2$

Overall cell: $CH_3COO^- + 4H_2O \rightarrow 2HCO_3^- + H^+ + 4H_2$

Solid Oxide Electrolysis

Anode: $O^{2-} \rightarrow \frac{1}{2}O_2 + 2e^-$

Cathode: $H_2O + 2e^- \rightarrow H_2 + O^{2-}$

Overall cell: $H_2O \rightarrow H_2 + \frac{1}{2}O_2$
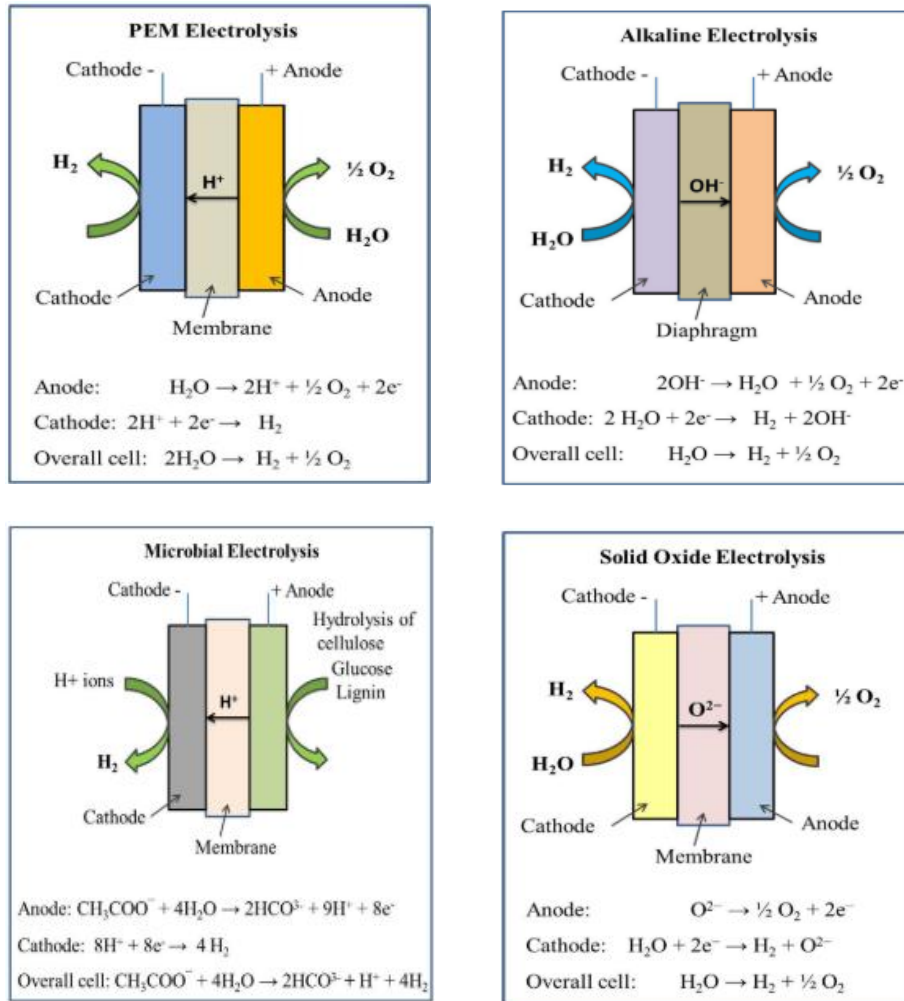
Figure 3. Four types of water electrolysis [72].

PEM electrolysers are available to be used but duo to their high cost and technology are more suited for low-scale applications. The electrolyte in PEM, is a gas-tight thin polymeric membrane where functional groups of the sulfonic acid type are present. An ion exchange mechanism takes place from the proton (H^+) conductivity of the materials. Nafion is the most used membrane for water electrolysis. The very low gaseous permeability of the membrane eliminates the risk of formation of flammable mixtures [73]. The high level safety that PEM water electrolysis is not the only advantage but also, the high current density and the possibility of changing/switching the operating modes between fuel cell and electrolyser [74].

Photo-electrolysis is a method that utilises light to provide the required energy for water splitting. During photoelectrochemical (PEC) water splitting a semiconductor material that is usually applied as a photo anode, or cathode depending on which reaction is in favour. When energy in

form of UV-visible light equivalent or greater than the semiconductors band gap is absorbed, an electron hole-pair is created on its surface that oxidise water into gaseous oxygen and hydrogen ions. The ions then travel to the other electrode through the electrolyte and get reduced to hydrogen gas from the photoexcited electrons at the conduction band [75, 76].

Hydrogen and oxygen gasses can be easily separated by a semi-permeable membrane [75]. Photo electrolysis possesses advantages such as its low cost, flexible size that allows small scale production but is limited by its relatively low solar to hydrogen conversion efficiency. In order for the efficiency to increase, extensive research needs to be carried out around new photocatalytic material since the main limitations of this process currently derive from the semiconductor. Several of the typical semiconductors are not efficient for this method since they do not react under visible light and even the ones that do like TiO_2, the most commonly used one, phase several other limitations that prevent the efficiency from reaching desirable numbers [76].

In order to identify the challenges for TiO_2 based photocatalysts with different morphological properties, Eidsvag et al. [77] carried out experimental and theoretical research concluding that there are non-standardised presentation of results, bandgap in the ultraviolet (UV) region, lack of contribution between experimental and theoretical work and lack of large/small scale production facilities. Park et al. [78] investigated characteristics of H_2 produced by photocatalytic water splitting using liquid phase plasma over Ag-doped TiO_2. Due to the properties of TiO_2 photocatalysts the rate of hydrogen generation is superior and its further increased with the addition of doped Ag, participation of liquid phase plasma and aqueous phase solutions containing CH_3OH additives. The injection of additive improved the optical properties by increasing the OH radical generation and the CH_3OH additive is decomposed to act as an electron donor.

Liu et al. [79] developed a water-stable metal-organic framework (MOF) to perform photocatalytic water splitting. A Ni-based MOF single crystal and its exfoliated nanobelts were studied and indicating that they can be applied in a wide range of pH environments. The observed experimental and theoretical results showed than electron transfer is feasible from the harvesting center to the catalytic center. Moreover, results showed that the exfoliated nanobelts had more efficient charge separation due to its shortened charge distance and enhanced active surface areas, resulting in 164 times of promoted water reduction activity.

3.2.3 Formic acid to hydrogen

FA, as a liquid organic hydrogen carrier, can be catalysed to hydrogen using metal and metal-complex catalysts using FA as a hydrogen donor, as well as fuels and electrical energy (Fig. 4) [80-85]. Cai et al. [86] investigated the dehydrogenation of FA using the $L1_1$-type ordered Pt-based intermetallic compounds (*i.e.*, X-Pt, X = Ag, Cu, Au, Pd, Ir, Rh, Tc, W, V). The results showed that there was a positive relationship between carbon monoxide (CO) and carboxyl (COOH) or hydrogen atom. However, a weak relationship with a negative slope for CO versus formate (HCOO) or CO versus hydroxyl (OH). This was credited to the beyond *d*-band-center model for the explanation of adsorption energies of HCOO and OH. The highest catalytic activity and selectivity for the decomposition of FA is observed by the L1$_1$-type CuPt catalyst.
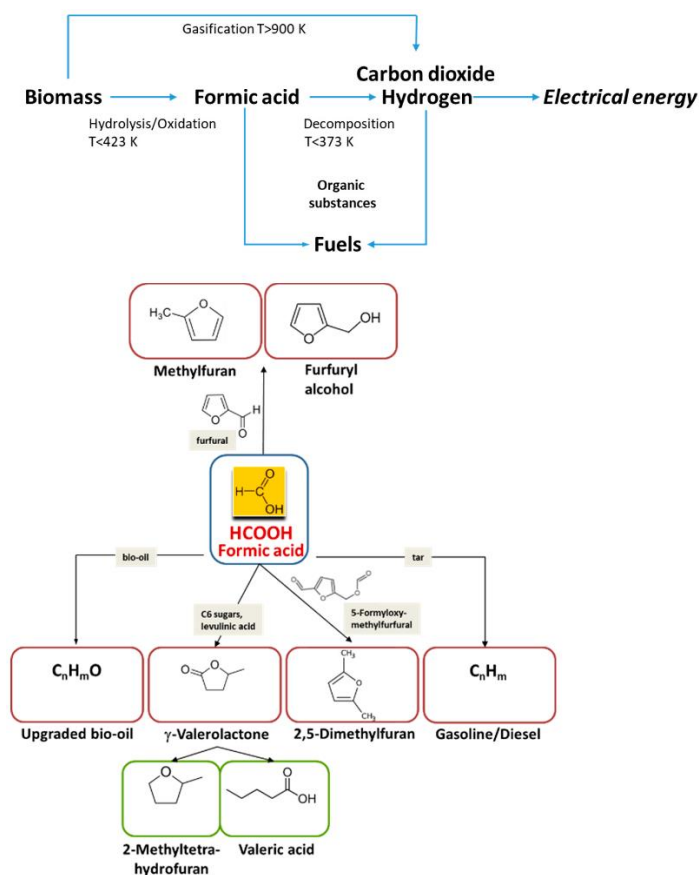
Figure 4. Schematic representing the generation of fuels and energy from formic acid obtained from biomass [80].

A further study conducted by Shaybanizadeh et al. [87] investigated boron nitride nanosheets supported on homogeneous bimetallic AuPd alloy nanoparticles catalyst for FA decomposition for

hydrogen production. The bimetallic Pd–Au alloy nanoparticles were effectively stabilized and uniformly distributed on boron nitride nanosheets (BNSSs) surface via the precipitation process. It was found that the catalyst accomplished a 100% selectivity under optimum reaction conditions (50 °C, 100 min, 20 mg cat., water solvent), with an average TOF of about 6848 h^{-1}. The authors concluded that these results should encourage future developments of bimetallic heterogeneous catalysts with high performance for the decomposition of FA.

Xu et al. [88] developed graphene nanosheets with nickel particles using reduced graphene oxide (RGO) self-assembly bonded nickel particles. The study aimed to facilitate the room temperature dehydrogenation of formic acid for hydrogen production by using a low-cost non-noble metal catalyst. The catalyst exhibited excellent performance during FA decomposition for hydrogen production, with a hydrogen yield of 240.0 mL g^{-1} h^{-1} at 50 °C. It was concluded that these results were similar to that achieved with majority active non-noble metal catalysts.

Recently, the photocatalytic water splitting for hydrogen production has recently been the most attractive option due to its cost effective, environmentally friendly, and pollution-free nature [89-92]. Suhag et al. [93] studied the photocatalytic production of hydrogen from FA using a solution with TiO_2. From the results, it was observed that the photocatalytic hydrogen production with TiO_2 by the simultaneous deposition of Rh was 5.0 mmol g^{-1}, 12.2 mmol g^{-1} and 16.0 mmol g^{-1} after 1 h, 3 h and 5 h of irradiation time for black light, respectively. Furthermore, it was observed that the photocatalytic hydrogen generation with the aid of the simultaneous photo-deposition of Rh metal on TiO_2 was approximately 250 times superior to that obtained with the bare TiO_2.

4. Catalysts for FA decomposition

4.1 Homogeneous catalysts

Ruthenium-based homogeneous catalysts have been effective for the decomposition of FA for hydrogen production. Gao et al. [94], investigated the dehydrogenation of FA using a homogeneous complex [$Ru_2(\mu$-CO)(CO)$_4(\mu$-dppm)$_2$] in acetone solution catalyst. For the first time, a binuclear homogeneous catalyst was successfully utilised for the decomposition of FA or the hydrogenation of CO_2 to FA.

A further study performed by Patra and Singh [95], studied water-soluble ruthenium complexes $[(\eta^6\text{-arene})Ru(\kappa^2\text{-L})]^{n+}$ ($n = $ 0,1) ([Ru]-1–[Ru]-9) ligated with pyridine-based ligands for the dehydrogenation of FA. The results showed that the [Ru]-1 catalyst also catalyzed the conversion of formaldehyde to hydrogen gas in water under base-free conditions. It was concluded that the current catalytic system can integrate FA dehydrogenation with formaldehyde dehydrogenation.

Furthermore, Boddien et al. [96], investigated the decomposition of FA using active Ru catalysts. The results showed that with the *in situ* generated $[RuCl_2(benzene)]_2$/6 equivalent (diphenyl-phosphino)ethane (dppe), the catalysts were shown stable and continuously operating for the decomposition of FA with the turnover frequencies (TOF) and turnover number (TON) at $900\ h^{-1}$ and 260000 under mild conditions. In addition, Gan et al. [97], used a homogeneous ruthenium-TPPTS catalyst to investigate its performance on a homogeneous and on a heterogeneous catalytic system, after the immobilisation of the catalyst. Fig. 5 shows the comparison between the recycling of homogeneous and heterogeneous catalytic systems. The 92nd reaction cycle could achieve a 95% conversion within 30 minutes, which was nearly the same as the homogeneous catalytic reaction (Entry 1). However, according to XRF spectra, when the solid catalyst was washed with water, Ru-TPPTS could be removed gradually, showing that the zeolites here were mainly used as physical absorbents. They ended up with the fact that with heterogeneous catalysts the separation of the catalysts from the solution is easier and the leaching of metal is negligible.
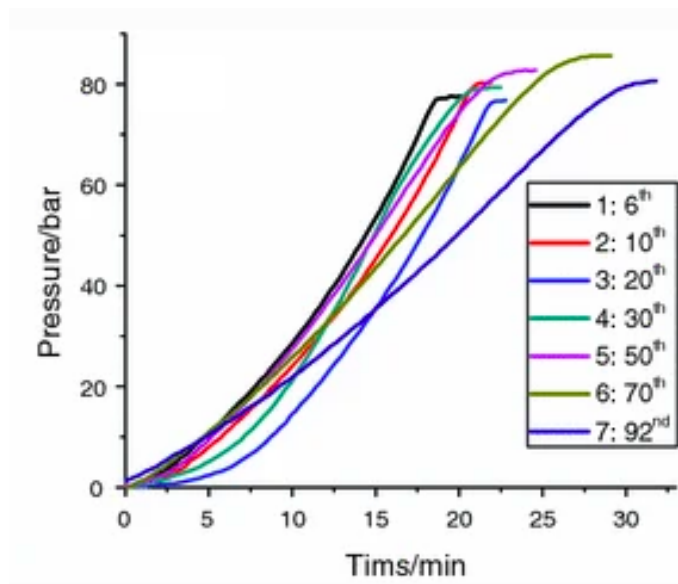
Figure 5. Comparison of kinetic curves of the experiments using the ruthenium-TPPTS catalyst in homogeneous and heterogeneous catalytic systems. Entry 1, 6th recycling experiment in an aqueous homogeneous solution; Entries 2-7, catalysts absorbed on zeolite [97].

Iridium-based catalysts have further shown promising results for FA decomposition. Barnard et al. [98], utilised cyclometallated iridium(III) complexes based on 2-aryl imidazoline ligands as effective catalysts for FA decomposition. The results showed that the catalyst was able to achieve TOF of up to 147 000 h^{-1} at 40 °C, with negligible production of CO. Furthermore, Guo et al. [99], applied a novel series of Cp^*Ir (Cp^*=pentamethylcyclopentadienyl) catalysts, incorporated with picolinamide-based ligands, for the dehydrogenation of FA. The findings showed that an increase in the electron density of amid N atoms could increase the system reactivity. It was concluded that the current system can attain a high TOF and TON of 90625 h^{-1}, 120520, respectively, at a temperature of 80 °C.

4.2 Heterogeneous catalysts

The heterogeneous catalysis of FA decomposition was initially studied in the gas-phase and then in liquid-phase due to the complexity of the system. Palladium (Pd) based catalysts favor the H_2 generation against the CO production [100]. Moreover, not only mono-metallic based catalysts, like Pd, gold (Au), silver (Ag), platinum (Pt), ruthenium (Ru) etc., but also, a complex of bi- and tri-metallic catalysts may be used [101].

Hu et al. [102], analysed the activity of a commercial Pd/C catalyst for FA's decomposition. They found out that reaction is depended by the nanoparticle size of the Pd and that more focus must be shown on the designing of the catalyst in order to avoid deactivation by the occupation of active sites.

Bulushev et al. [103], compared the activity of Au/C and Au/N-C catalysts with Au/SiO_2 and Au/Al_2O_3. The Au catalyst supported on N-doped carbon has shown the best catalytic activity at 448 K, but not the highest H_2 selectivity. According to the TEM analysis, the difference in dispersion and the fact that the breakage of C-H bond in formate species on the single Au atom takes place more easily at Au/N-C can explain the high activity of the catalyst. Chesnokon et al. [104], investigated a new catalytic system Pt/N-graphene system for the FA decomposition

reaction. Graphene powders doped and undoped with nitrogen atoms were studied and again it was concluded that the presence of nitrogen atoms in the catalysts increased the catalytic activity and herein the conversion to the route of H_2 and CO_2.

Faroldi et al. [105], studied the performance of Ni, Cu and Ni-Cu catalysts supported on a high surface area graphite doped with alkali oxides and undoped. The Ni-Cu/K catalyst showed the best performance at 130 °C with 100% conversion of FA and 95% selectivity of H_2. It was concluded that formate, bicarbonate, or carbonate species decomposed at different temperatures depending on the alkali metal in the catalyst.

Trimetallic nanoparticles composed by Ni, Au and Pd supported on amine-functionalized carbon nanotubes were developed to study their activity on FA decomposition by Zhang et al. [106]. The high catalytic performance of the catalyst is attributed to the high dispersion of nanoparticles and the boost effect of $-NH_2$ group on O-H cleavage. The NiAuPd/NH_2-CNT catalyst and the NiAuPd/NH_2-CNT-S, which is a result from the electronic synergistic effect of the three metals by the formation of electron-rich Pd surface, can promote the application of FA's decomposition in fuel cells giving 100% H_2. Fig. 6 depicts the mechanism for formic acid decomposition over the current catalyst.
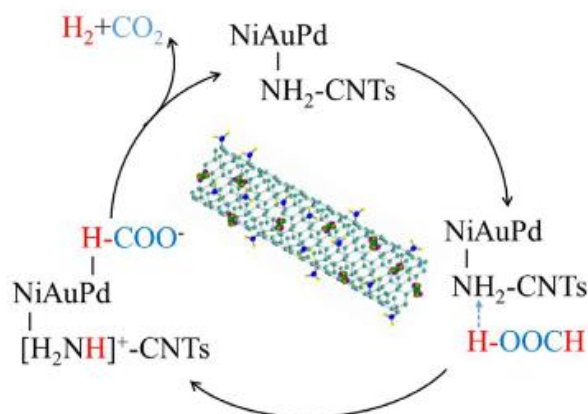
Figure 6. Schematic illustration of plausible mechanism for the decomposition of FA over NiAuPd/NH_2-CNTs [106].

4.3 Structural and physicochemical properties of heterogeneous catalysts

Despite the kind of metals that are involved in the efficiency of a reaction, the structural and physicochemical properties of catalysts are key factor to achieve higher yields. Yang et al. [107] performed a comprehensive study, on previous experimental data in order to investigate the relationship between the structure of Pd-based alloy catalysts and their catalytic activity for FA decomposition. Five atomic arrangements are considered, including an overlayered structure, core-shell structures of Pd/M and Pd/Pd-M, a uniform alloy and a subsurface structure (Fig. 7). Based on Sabatier analysis, the CO and OH adsorption energies are correlated with the activity and selectivity for FA decomposition, with the average Bader charge of Pd atoms on the surface and the average bond length of surface atoms are key factors for adjusting adsorption energies of CO and OH. According to the proposed strategy, two surface structures, i.e., $Pd_{2L}@Pd_1Ag_1$ and $Pd_{2L}@Pd_1Au_1$, are predicted to be promising catalysts for highly selective FA dehydrogenation.
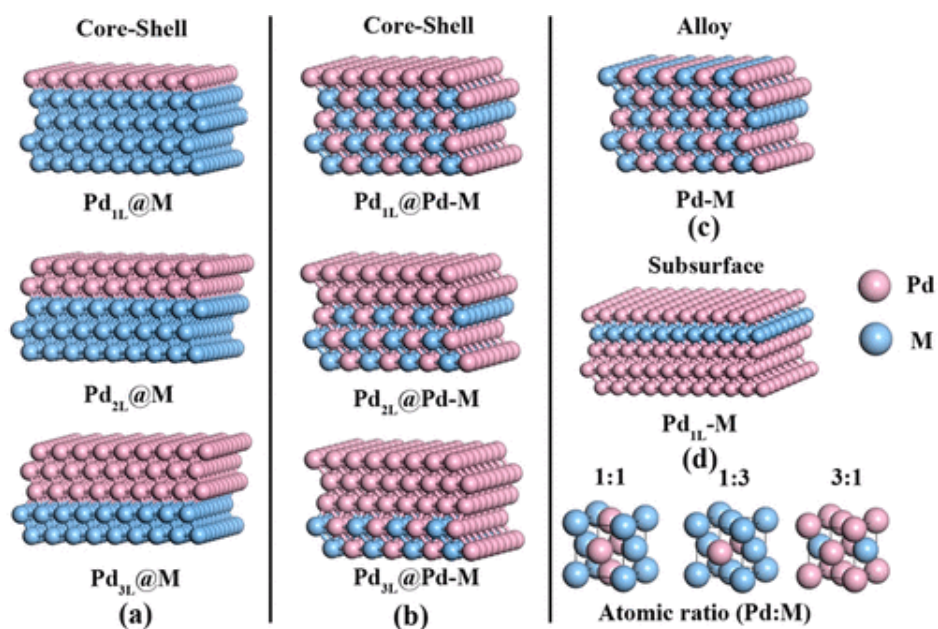
Figure 7. Models for the surface structures: (a) core-shell with Pd-M, (b) core-shell with Pd alloy, (c) alloy, and (d) subsurface [107].

The need to prepare Pd/C catalysts with high efficiency, minimum formation of CO and stability remains a grand challenge that we need to overcome. Sun et al. [108] developed a catalyst of ultrafine Pd particles uniformly embedded in N-enriched mesoporous carbon (Pd/NMC) by integrating N-doping, mesopore confinement and small size effects into one composite. Pd nanoparticles were distributed in a narrow range of 1.2 – 1.4 nm and evenly dispersed on the NMC

with high dispersion of 90% – 96% compared to Pd/MC who had a larger size and non-uniform dispersed Pd. The strong interaction between Pd- and N-containing functionalities and the ultrafine and small-sized Pd particles increased the activity of the catalyst over 12 times and also improved the cycle performance. Also, it was observed that the temperature effect decreased the total N and surface pyridinic N content, though in the lowest temperature (400 ^{o}C), Pd/MCP had lower surface area and larger-sized Pd particles and it showed higher catalytic TOF.

The activity of Pd-Ag catalysts was examined by Sneak-Platek et al. [109]. The results showed that the surface area was not affected significantly by the temperature treatment of the catalyst nor by the preparation method used. In most cases, the BET surface area ranged between 95 and 114 m^2/g and was only slightly lower than the one for AlOOH, with similar results to be obtained for pore volume and radius of the catalyst. DFT computational study showed that Pd is active but prone to poisoning by CO, which is limited on diluted Pd-Ag alloy with strong intermetallic interactions, where the CO adsorption is very weak thanks to the isolation of Pd atoms.

Santos et al. [110] studied the size-activity dependence of Pd based catalysts in FA dehydrogenation reaction. A wide range of particle sizes (2.8 – 56 nm) were prepared upon various synthetic parameters, precursor and solvent nature resulting diverse in activity towards hydrogen production. Acetone prepared catalysts resulted smaller particles than water-mediated homologous and these catalysts with smaller Pd sizes showed superior catalytic performance. Specific rate and TOF calculations showed a maximum value for specific activity situated around 4 – 5 nm in a volcanic-type relation. In addition, the guiding factor for activity is the low/high coordination atoms ratio.

4.4 Carbon formation

Carbon formation from C-containing gases has been an important concern for industries where in most of cases the carbon formation is associated with the deactivation of catalysts. C-H bond and C=O bond of various gases such as CO_2 and CH_4, are hard to break, though the catalysts by decreasing the activation energy can make feasible an undesirable formation of carbon [111]. The selection of suitable catalysts is a crucial factor for H_2 generation. Ni-based catalysts have been widely applied at industrial level due to their low cost and high activity but suffer from coke formation during steam reforming [112]. High temperatures favor the carbon deposition since bond between the atoms of molecules are easily broken. Charisiou et al. [113] investigated the effect of

temperature and carbon formation on Ni-based catalysts of biogas dry-reforming. The results showed that carbon formation and metal particle sintering had led to the deactivation of catalysts. Also, the reduction on the performance of each catalyst is more significant after 2-3 hours of time-on-stream. At higher temperatures the CO production is enhanced where the decomposition of CO is responsible for the coke formation.

Graschinsky et al. [114] presented a thermodynamic study of the autothermal ethanol reforming process for H_2 production. CO content in the obtained mixture is desirable to be low to reduce purification costs. In fact, increasing the water content in the feed decreases the CO content while the WGS reaction is taking place. On the other, carbon deposition onto the active sites of catalyst causes a decrease in the activity of the catalyst and/or increase the reactor pressure drop making impossible the process to continue. However, according to the thermodynamic study lower temperatures and water to ethanol ratios lower than 4 favour coal formation. Also, the effect of the addition of O_2 in the feed contributed to reduce carbon formation.

Both gasification and pyrolysis processes generate chars and tars during biomass conversion. Therefore, it is important to eliminate their presence since they occur deactivation to the catalysts used for these processes. During the steam reforming of biomass, two types of carbon are formed, whisker and pyrolytic. Whisker carbon is typically formed at 500 – 600 $^{\circ}$C while pyrolytic carbon is enhanced at temperatures over 600 $^{\circ}$C [115]. Kihlman and Simell [116] investigated the gasification gas of biomass that was then converted to CO and H_2. For the reforming of these gases Ni- and Rh-based catalysts were used with the first one promoting more the coke formation. Only on the Rh-based pressure increased the carbon formation possibly due to carbon oxidation reaction or promoted reaction of carbon formation in contract with the other catalyst. In addition, no whisker carbon was detected with the carbon formed being characterized as encapsulating and, graphitic content was found to be high compared to amorphous.

Bio-oil derived from the pyrolysis of biomass can be further treated to be used as biofuel, but due to the heating needed for the process the bio-oil induces the polymerisation and cracking to produce coke [117]. Li et al. [118] studied and reported a mechanism for the coke formation of a Ni/HZSM-5 and Ni-Cu/HZSM-5 catalysts for rice husk bio-oil hydrodeoxygenation. The main reason for the deactivation of N/HZSM-5 is that soluble coke was formed on the Brønsted acid sites of the support while the addition of Cu showed higher resistance to coke graphitization. On

these active sites the reactions of functional groups in bio-oil occurred while the dehydration of compounds significantly contributed to the coke formation. Moreover, from the coke particle sizes formed on the surface of catalysts it was concluded that Ni/HZSM-5 is deactivated from the formation of graphitic carbon and in contrast, Ni-Cu/HZSM-5, who had smaller coke particle sizes, was deactivated due to oxygenated hydrocarbons on the surface of catalyst.

Similarly, with H_2 production from fossil fuels and biomass, the formation of CO during FA decomposition inhibits the activity of catalysts. Li et al. [119] studied the formic acid decomposition that was selected to investigate the mechanism of bio-oils catalytic reforming. Density functional theory calculations studies were performed coupled with microkinetic modeling. The results showed that the formation of -COOH is kinetically the most preferred reaction which is then decomposed to CO and CO_2. The direct formation of CO has an activation barrier of 0.51 eV and was associated with a strong exothermicity of -1.20 eV, which leads to its dramatic thermodynamic preference. The combined with the kinetics model reveal that on the stepped Ni surface, COOH and CO are the two dominant products from FA.

Hafeez et al. [120] developed a CFD model in order to investigate the performance of a Pd/C catalyst and in addition the deactivation of the catalyst. CFD and experimental results showed both that the conversion decreases rapidly after 75 minutes and then continues to do so steadily with time which is might due to the deactivation of catalyst. The cause of deactivation was then evaluated leading to claim that CO is the poisoning molecule which can absorb stronger on Pd than CO_2 and H_2. A demonstrated sound validation, for the first time, was developed of the CFD model with the experimental results that can successfully predict the deactivation of Pd/C. Fig. 8 depicts the conversion of formic acid against time. According to catalyst reusability studies, the catalyst can be restored for 10 times without any reduction to its activity. Sanchez et al. [121]examined the dehydrogenation of FA using a commercial Pd/C catalyst investigating its catalytic activity and stability. The stability of the catalyst was investigated at catalytic cycles of 1.5 hours each revealing that at the 5th catalytic cycle, Pd/C catalyst preserved 72% of its initial activity. It was concluded that the slight deactivation of catalyst was probably due to the strong absorption of FA on the catalytic surface, agglomeration of Pd particles, poisoning from CO, or decrease of Pd loading by leaching.
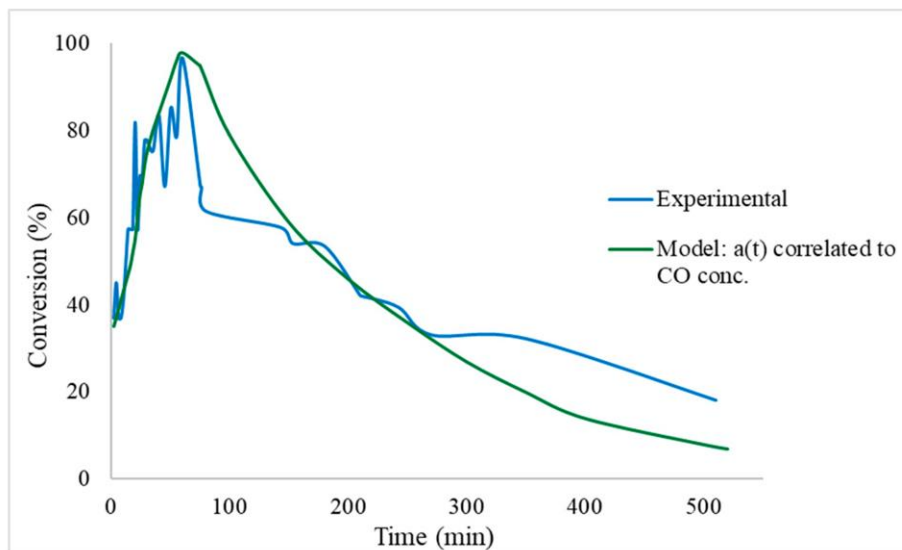
Figure 8. Conversion of formic acid against time with catalytic activity correlated to CO concentration in microreactor [120].

5. Reactors

Hydrogen from FA is conventionally generated using fixed bed reactors. These reactors are widely known and used for their heterogeneous catalysed gas or liquid phase reactions, where catalyst particles are loaded in the bed and are in direct contact with FA [122]. Fixed bed reactors are suitable for exothermic reactions, due to their high heat transfer [123]. In order to optimise the reaction system, the dehydrogenation of FA has been performed and in other reactors, such as stirred tank reactors (continuous and batch) and microreactors. Stirred tank reactors are used a lot at industrial scale for both homogeneous and heterogeneous reactions. In many cases, there is more than one phase and mixing may be required [124]. Continuously stirred tank reactors (CSTRs) play a crucial role in maximising the productivity of chemical processes; however, due to their highly non-linear dynamic and sensitivity, it is difficult to analyse and control such systems [125]. In contrast, batch reactors are most often used for low production capacities, where the cost of labour and dead time are only a small fraction of the unit cost of production [126]. Microstructured reactors are recently developed and are very promising and attractive to scientists especially for enhancing mass and heat transfer [127]. Table 1 displays a quantitative analysis of the types of reactors utilised for FA decomposition to produce hydrogen.

**Table 1.** Types of reactors utilised for the decomposition of FA.

Reactor	Catalyst	Temp. (K)	X_{FA} (%)	H_2 selectivity (%)	H_2 yield (%)	Ref.
Fixed bed reactor	2% Ir/Norrit	473	100	99.5	99.5	[128]
Fixed bed reactor	1% Mo_2C/Norrit	473	100	100	100	[129]
Fixed bed reactor	1%Pd/C	523	78	97	75.6	[130]
Fixed bed reactor	10%Mo_2C-0.5%Co/GAC	423	91.6	99.7	91.3	[131]
Fixed bed reactor	Ni/Ca(19.3)-SiO_2	433	100	92	95	[132]
Fixed bed reactor	Pd/ZnO	473	19	99.3	18.8	[133]
Fixed bed reactor	Au/TiO_2	463	100	5	5	[134]
Batch reactor	2% Pd_6Zn_4	303	75	-	-	[135]
Batch reactor	1% pd/γ-Al_2O_3	293	60		35	[136]
CSTR	TiO_2 film	340	96	-	-	[137]
CSTR	Pd/C	323	~80	-	-	[138]
PFR	Pd/C	323	10	-	-	[138]
Microchannel reactor	1.15% Au/Al_2O_3	623	98	70	68.7	[139]
Microreactor	Soy-Mo	333	80	100	80	[140]
Microreactor	Mg-MoC	473	92	-	-	[141]
Packed bed microreactor	Pd/C	303	33	-	-	[120]
Batch microreactor	Pd/C	303	29	-	-	[120]
Packed bed microreactor	Pd/C	303	9.1	-	-	[142]
Coated wall microreactor	Pd/C	303	9	-	-	[142]
Membrane microreactor	Pd/C	303	48.6	-	-	[142]

5.1 Fixed bed reactors

The most common and well-studied reactor for the decomposition of FA is the fixed bed reactor since many scientists usually use them in order to study the performance and the catalytic activity, stability of various catalysts. It well known that they play a key role for heterogeneous catalysis. The radius of packed bed reactors is usually small due to the transfer of heat into or out of the system from the strong endothermic or exothermic surface reactions [123]. For the decomposition of FA to a CO-free effluent, over supported Pt metals [128], and Mo_2C catalysts [129], a continuous flow fixed bed reactor was used with the reaction to take place in vapor-phase. The reaction conditions for these two types of catalysts were similar. The reaction took place at atmospheric pressure, the flow rate was 40 ml/min and Ar gas was used as carrier, which was bubbled with the FA at room temperature. The decomposition of FA over the Pt metals started at and above 350 K with the production of CO-free H_2 only to be achieved on one of the studied catalysts (Ir/carbon Norit) and not on Pt metals deposited on carbon Norit. Moreover, in order to improve the selectivity of H_2 of all the other catalysts, they added water to FA. The supported Mo_2C was prepared by the reaction of MoO_3, with the highest H_2 yield to be obtained on 1% Mo_2C/carbon Norit without the presence of water. The addition of water, therefore, improved the selectivity of H_2 by eliminating CO from the products on all the carbon supported Mo_2C.

The catalytic decomposition of FA to H_2 in a laboratory scale fixed-bed reactor was studied theoretically and experimentally by Winkler et al. [130]. The operation conditions of the reactor were 150-225 °C and 1 atm. The catalyst was palladium deposited on porous active subunit (Pd/C) with the mass limitations to be negligible. They also showed that the effluent contained negligible amounts of CO and that the multistep model they suggested where the adsorption and dissociation mechanism was included, had a good fit with the experimental results. Fig. 9 shows the process flow diagram (PFD) of the experimental setup.
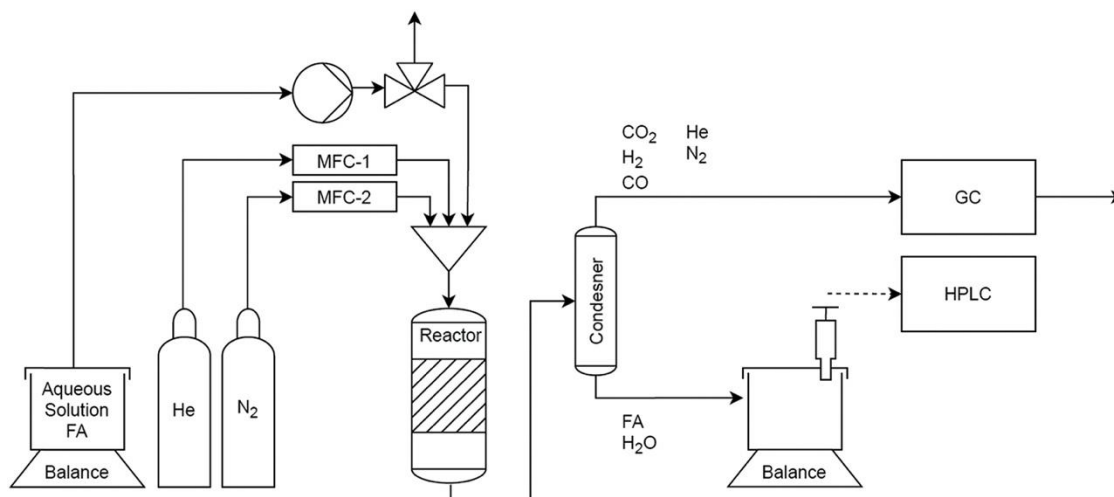
Figure 9. Process flow diagram of the experimental setup for FA decomposition [130].

Zhu et al. [131], also studied the H_2 production from FA on MoC_2 and metal doped MoC_2 on granular activated carbon (GAC) catalysts under mild reaction conditions in a laboratory scale fixed bed reactor. Metal doped catalysts showed better results than the MoC_2/GAC, with the MoC_2-Co/GAC to achieve the highest H_2 selectivity of 99.7% and FA conversion of 91.6% at 150 °C, being the doubled conversion compared to MoC_2/GAC catalyst at the same temperature. H_2 selectivity of all the catalysts were high and above 90%.

The effect of calcium content for the H_2 generation via the dehydrogenation of FA in a conventional fixed-bed flow reactor was investigated by Faroldi et al. [132]. The catalysts were used for the FA decomposition were Ni supported on SiO_2 and on Ca-SiO_2 with the concentration of Ca varying between 3.4 - 19.3 wt%. The highest Ca content catalyst (19.3 wt%) was the one that showed 100% conversion of FA at 160 °C, with this being 20 °C lower than the Ni/SiO_2.

Bulushev et al. [133], were one of the firsts who studied the FA decomposition over Pd/ZnO catalysts in a packed bed reactor In their study they investigated the performance of the new catalyst compared to Pt/ZnO, Pd/Al_2O_3 and ZnO catalysts. The Pd/ZnO catalyst might showed the second highest conversion in comparison with the other catalysts but had the highest selectivity due to the formation of PdZn alloy during the pre-treatment of the catalysts. Also, the activity of Pd/ZnO catalyst was higher than Pt/ZnO and ZnO but did not differ from that of Pd/Al_2O_3.

Sobolev et al. [134] investigated the presence of gold as a support material on nanoparticles for FA's decomposition in a gas flow packed bed reactor. The catalysts were used are, Au/TiO_2,

Au/SiO$_2$, and Au/Al$_2$O$_3$ and compared for their catalytic activity. Au/TiO$_2$ showed the highest FA conversion at low temperatures compared to the other catalysts, but the selectivity of H$_2$ was significantly low (< 20%). The other two gold supported catalysts showed better results on hydrogen's selectivity. The presence of gold nanoparticles targets the desirable pathway to give H$_2$ rich gas depending the nature of the support.

5.2 Stirred tank reactors

Continuous flow reactor can cope with higher reactant concentrations, can achieve greater separations between reactants and products and has more flexibility on operation when compared to a batch reactor [143]. Both are often used for liquid-phase reactions; however, batch reactor is used in low scale reaction systems. Also, in a batch reactor is not possible to study detailed the catalytic activity of a catalyst and the operating cost is higher than of a continuous system, so, the usage of batch reactors as fuel cell systems is limited. Fig. 10 shows the CSTR for the continuous generation of H$_2$ from FA.
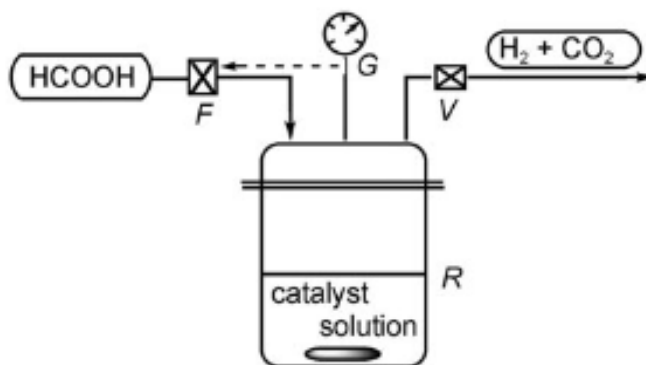
Figure 10. Schematic arrangement for the continuous generation of H$_2$ from FA. *R*: stirred tank reactor with heating/cooling; *G*: pressure gauge/transducer; *F*: flow control valve; *V*: gas release valve [9].

Hafeez et al. [135], investigated the decomposition of FA under mild conditions using a 2% Pd$_6$Zn$_4$ catalyst in a batch reactor. The effects of temperature and FA concentration on the conversion of FA were studied. The increased temperature and concentration improved the decomposition of FA while, the experimental and simulated results showed good match. The studied catalyst was then

compared with a commercial Pd/C catalyst, with the bimetallic catalyst to enhance the decomposition of FA.

Xu et al. [136], investigated the activity, selectivity, and the effect of oxygen on FA decomposition using Pd/γ-Al_2O_3 catalyst in a 1 L batch reactor operated at 20 °C and atmospheric pressure. In the gas products only H_2 and CO_2 were detected and produced in equal amount in agreement with the stoichiometry of the reaction, with a small delay in the first half hour since the concentrations of H_2 and CO_2 in the gas cap must build up first. Initially the reaction rate was constant, but the reaction became extremely slow after 1 hour. The presence of O_2 (0 – 2 vol%) enhanced the conversion of FA and the production of CO_2. In contrast, the H_2 yield reached a maximum at 0.1 vol% of O_2 and then decreased exponentially. The catalyst activity was tested for 4 hours by adding every 60 minutes the same amount of FA in the presence of inert (Ar) gas and in the presence of 0.1 vol% O_2. Under the inert gas the reaction rate decreased even more after every adding dose of FA, but under the oxygen's presence the catalyst maintained its activity in three runs, showing a small deactivation.

Zhao et al. [144], studied, at room temperature, the decomposition of FA on monometallic Pd and Au and bimetallic Pd metal supported gold nanoparticles in a semi-batch reactor. Pd content increased the catalytic activity with the 300 sc% (calculated in terms of Pd surface coverage) Pd-on-Au/C to generate 58.2 L of gas in 3h with no deactivation of the catalyst. Also, the presence of Pd favored the elimination of CO formation. The nanoparticle size of Pd is important for the chemisorption geometry of the formate species and for the surface reaction pathway.

The photocatalytic decomposition of FA over TiO_2 thin film catalyst in a CSTR was investigated by Ellwood et al. [137]. A non-stationary dynamic model was proposed including the FA adsorption, the desorption steps, the formation of catalytic active sites and the decomposition of the adsorbed species over the catalyst. A computationally aided nonlinear frequency response (cNFR) method was used to analyze the reactor's response to the modulation of the four inputs. The optimized model improved, therefore, the FA conversion to 96%.

Caiti et al. [138], investigated experimentally the hydrogen production from FA on a commercially Pd/C catalyst. The kinetic model included studies in plug-flow reactor (PFR) and in CSTR, with the last one being capable to achieve H_2 generation for over 2500 substrate turnovers without losing activity when the rate of FA addition and decomposition were equals. In the PFR the catalyst

particles were poisoned and deactivated due to the adsorption of FA on the surface of the metal. The increased stability in the CSTR caused the increasing of the conversion of FA. Despite the superior performance of the CSTR in terms of stability and overall productivity, the lower catalyst to volume ratio and the decreased steady state concentration of FA do compromise the initial space time yield of the reactor by order of magnitude. Fig. 11 shows the comparison of Pd/C catalyst performance during FA decomposition in CSTR and PFR.
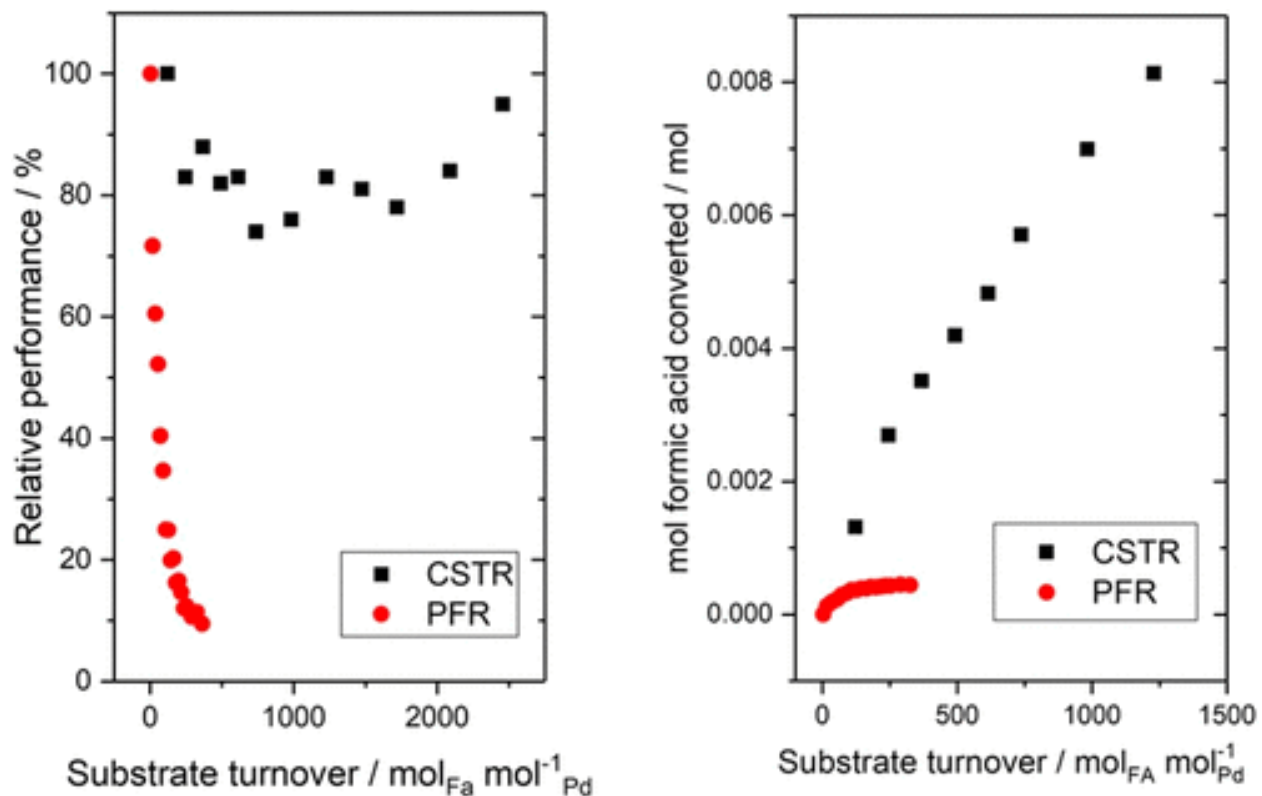
Figure 11. Comparison of Pd/C catalyst performance during FA decomposition in CSTR and PFR. (a) Relative performance of substrate turnover and (b) cumulative moles of FA converted in the two systems as a function of substrate turnover [138].

In contrast to PFRs, in CSTRs is seemed to be avoided the deactivation of the catalysts. Furthermore investigations, will compare the performance and stability of various catalysts in both reactors and efficiency of the regeneration of the catalyst in PFRs through thermal treatments.
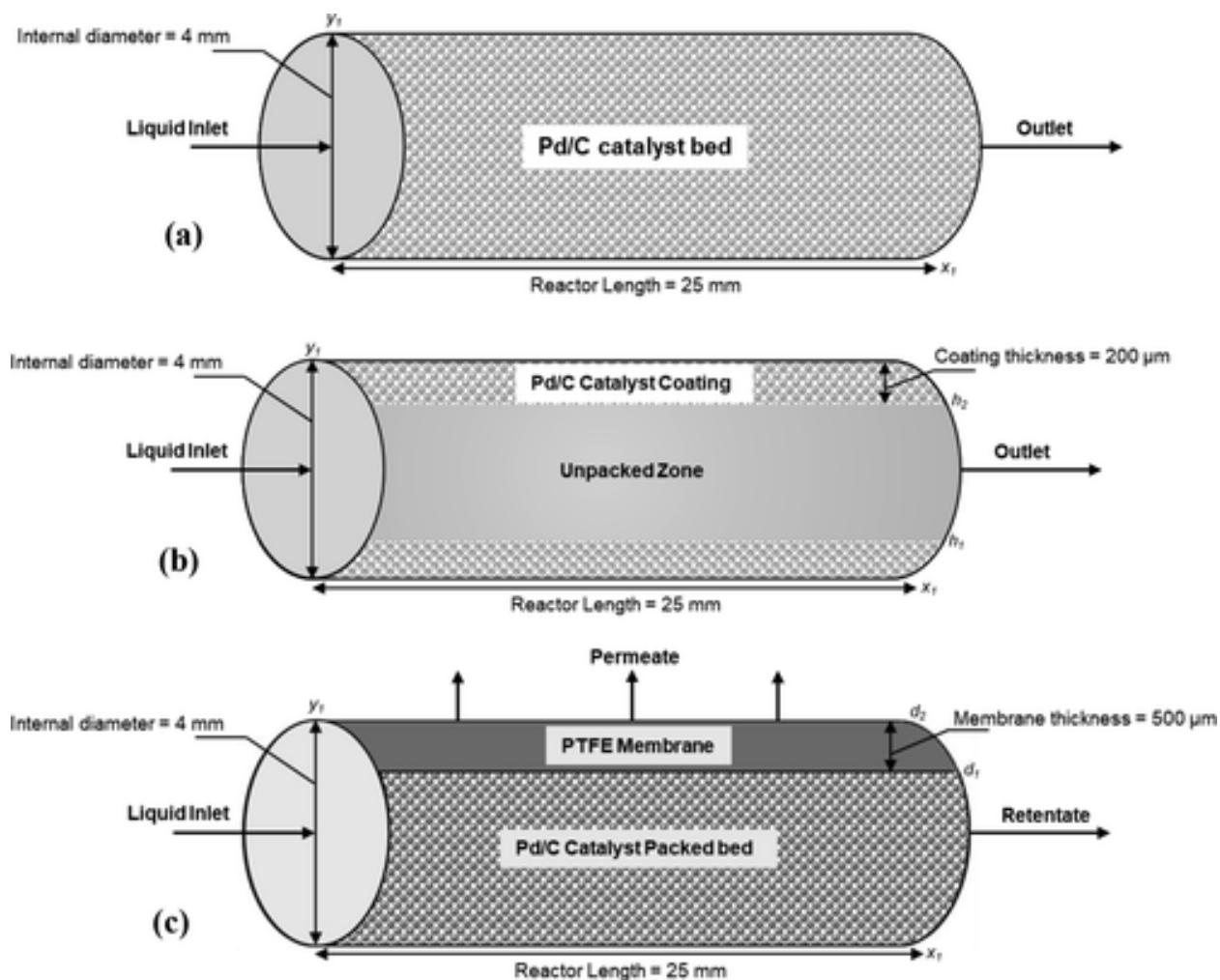
5.3 Microreactors

Microstructured reactors appear to be an alternative and promising technology the recent years with a lot of advantages. Their low structure cost, high heat and mass transfer and low-pressure drop have made microreactors attractive to scientists [127, 145]. Moreover, their high efficiency is also caused by the large surface they have to volume ratios while limiting the diffusion lengths. Few are the scientists who have studied FA's decomposition in microreactors. Ndlovu et al. [139], investigated the effects of temperature, inlet flow rate and the ratio of pure and diluted FA in feed on a demonstrated microchannel reactor for H_2 generation over a heterogeneous catalyst (Au/Al_2O_3) at reactor temperatures of 250-350 °C. At its highest temperature the FA conversion was found to be near to the equilibrium (>98%). Moreover, at 350 °C with flow rate 48 mL/min, the H_2 production was maximized, and the results showed that the H_2 yield was 68.7%. For the diluted feed of FA in water (50/50 vol%), the decomposition of FA to H_2 was more favored with the obtained selectivity of H_2 to be 81%.

Wang et al. [140], examined the decomposition of FA using a high-performance non-precious metal molybdenum-based catalyst near its boiling point, 110 °C, in a microstructured reactor. Even at such a low operating temperature the FA showed high conversion, up to 80%, with 100% selectivity on H_2. The high activity and stability of catalysts are due to the presence of non-ignorable K, the uniform dispersion of molybdenum species and the high basicity. Since the catalysts were prepared with different weight ratios of raw materials, at lower reaction temperatures the CO formation is affected.

Wang et al. [141], investigated the performance of various metals (Ni, Co, Mg, Cu, Ag) doped on nanosheet-like MoC catalyst in a microreactor with 6 mm inner diameter. The catalytic test took place at temperatures between 100-350 °C and atmospheric pressure with the Mg-MoC to be the most suitable catalyst for the reaction in terms of FA conversion and H_2 selectivity. In addition, the conversion was improved when the molar ratio of Mg:Mo was 1:100, however further increase to the loading amount of Mg decreased the conversion. The catalytic stability test of the catalyst performed at 200 and 300 °C showing excellent activity and stability for over 50 and 35 hours, respectively, for the FA decomposition.

Hafeez et al. [120], examined the performance of a packed bed and batch microreactor for the decomposition of FA using Pd/C catalyst. Results showed that the packed bed microreactor

achieved slightly higher conversions comparing with the batch microreactor, with the difference between the conversion of the two microreactors to be less than 10% and it can be assumed that they have similar performance. Moreover, they were the first to assess the performance of packed bed, coated wall, and membrane microreactors (Fig. 12) for the generation of H_2 using the same catalyst, under mild reaction conditions [142]. Experimental and simulated results were both discussed with the membrane microreactor having the best performance. Hydrogen's production was found to be lower in the packed bed microreactor when compared to the membrane reactor, because of the higher production of CO. Also, the coated wall microreactor required less amount of catalyst to obtain the same conversion with the packed bed microreactor. Negligible internal and external mass transfer limitations were found for all three microreactor configurations.

Figure 12. Representation of (a) fixed bed, (b) coated wall, and (c) membrane microreactors developed for the CFD modeling study [142].

As referred above the most common used reactor for the formic acid reaction is packed bed reactor. The pressure drop in fixed bed reactor is more significant at high flow rates and a less efficient heat removal as obtained with wall reactors. For that reason, microstructured fixed bed reactors can be applied in research and for small scale production only [146].

6. Conclusions and outlook

The environmental impact of convectional energy sources is increased year by year. The climate change has been a concert for scientists trying to find alternative and environmentally friendly raw materials for energy production. Therefore, in this review, the production of H_2 from fossil fuels and renewable sources is presented. H_2 is one of the greenest energy sources that can be used to provide engines with power. Currently, more than 95% of the global hydrogen supply is obtained from non-renewable sources, such as coal and natural gas, emitting harmful greenhouse gases. As a result, it is imperative to explore low-carbon methods of producing hydrogen to minimise the harmful environmental impact. One of the most promising liquid hydrogen storage chemicals is formic acid. The formation, transportation and decomposition of FA are easy to perform processes for hydrogen production. Heterogeneous catalysts are more preferable for this reaction causing less problems in contrast with the homogeneous catalysts. This review has investigated the decomposition of FA to H_2 rich gas in range of various reactors and presented a range of homogeneous and heterogeneous catalysts that have shown promising activity and stability, which is a key aspect for future commercial applications. The most common used reactor for the decomposition of FA is the fixed bed reactor. The packed bed with pellet particles and the high efficiency of mass and heat transfer allowed scientists to study the performance of new discovered catalysts in packed bed reactors. Tank reactors, and more specifically batch reactors may can be used to examine in detail the activity of catalysts, but it can be applied in low scale systems. On the other hand, CSTRs continuously decompose FA to H_2 and showed better performance in accordance with the stability of catalysts. The benefits of microreactors in contrast with macrostructured reactors are well known and their application on the decomposition of FA has been made the recent years. The performance of various kinds of microreactors are lacking from research so further research investigations are needed to compare with packed bed microreactors and their scalability to produce fuels on large scale. Future developments should be focused on the recovery of CO_2 to produce formic acid via hydrogenation. Furthermore, carbon formation has

been an issue with the catalysts applied for FA decomposition. Future work should explore the development of catalysts to prevent carbon formation and to move from batch to continuous systems with high activity and stability. One of the most challenging concepts for the future, is the development of catalysts of lower economical cost by decreasing the usage of noble metals, along with the concept of single-atom-catalysis that can develop catalysts with high exposure of active sites, nearly to 100% of the active sites and high thermal stability. Furthermore, life cycle assessment (LCA) studies should be performed in detail for FA synthesis, as well as FA decomposition for the production of hydrogen.

References

1.   Wang, X., et al., *Recent progress in hydrogen production from formic acid decomposition.* International Journal of Hydrogen Energy, 2018. **43**(14): p. 7055-7071.

2.   Meloni, E., et al., *Electrified Hydrogen Production from Methane for PEM Fuel Cells Feeding: A Review.* Energies, 2022. **15**(10): p. 3588.

3.   Ferraren-De Cagalitan, D. and M. Abundo, *A review of biohydrogen production technology for application towards hydrogen fuel cells.* Renewable and Sustainable Energy Reviews, 2021. **151**: p. 111413.

4.   Turner, J.A., *Sustainable hydrogen production.* Science, 2004. **305**(5686): p. 972-974.

5.   Moriarty, P. and D. Honnery, *Hydrogen's role in an uncertain energy future.* international journal of hydrogen energy, 2009. **34**(1): p. 31-39.

6.   Moriarty, P. and D. Honnery, *A hydrogen standard for future energy accounting?* international journal of hydrogen energy, 2010. **35**(22): p. 12374-12380.

7.   Felderhoff, M., et al., *Hydrogen storage: the remaining scientific and technological challenges.* Physical Chemistry Chemical Physics, 2007. **9**(21): p. 2643-2653.

8.   Alazemi, J. and J. Andrews, *Automotive hydrogen fuelling stations: An international review.* Renewable and sustainable energy reviews, 2015. **48**: p. 483-499.

9.   Joó, F., *Breakthroughs in hydrogen storage—formic acid as a sustainable storage material for hydrogen.* ChemSusChem: Chemistry & Sustainability Energy & Materials, 2008. **1**(10): p. 805-808.

10.   Eppinger, J.r. and K.-W. Huang, *Formic acid as a hydrogen energy carrier.* ACS Energy Letters, 2017. **2**(1): p. 188-195.

11.   Boddien, A., et al., *Towards the development of a hydrogen battery.* Energy & Environmental Science, 2012. **5**(10): p. 8907-8911.

12.   Grasemann, M. and G. Laurenczy, *Formic acid as a hydrogen source–recent developments and future trends.* Energy & Environmental Science, 2012. **5**(8): p. 8171-8181.

13.   Mellmann, D., et al., *Formic acid as a hydrogen storage material–development of homogeneous catalysts for selective hydrogen release.* Chemical Society Reviews, 2016. **45**(14): p. 3954-3988.

14.   Singh, A.K., S. Singh, and A. Kumar, *Hydrogen energy future with formic acid: a renewable chemical hydrogen storage system.* Catalysis Science & Technology, 2016. **6**(1): p. 12-40.

15.   Bhaskaran, R., B.G. Abraham, and R. Chetty, *Recent advances in electrocatalysts, mechanism, and cell architecture for direct formic acid fuel cells.* Wiley Interdisciplinary Reviews: Energy and Environment, 2022. **11**(2): p. e419.

16.   Mardini, N. and Y. Bicer, *Direct synthesis of formic acid as hydrogen carrier from CO2 for cleaner power generation through direct formic acid fuel cell.* International Journal of Hydrogen Energy, 2021. **46**(24): p. 13050-13060.

17.   Hossain, S., *Heteroatom-Doped Carbon Materials as Support for Anode Electrocatalysts for Direct Formic Acid Fuel Cells.* Int. J. Electrochem. Sci, 2021. **16**: p. 150926.

18.   Zhou, Y., et al., *Novel Superaerophobic Anode with Fern-Shaped Pd Nanoarray for High-Performance Direct Formic Acid Fuel Cell.* Advanced Functional Materials, 2022: p. 2201872.

19.   Zhang, L.Y., et al., *Synthesis of Palladium–Tungsten Metallene-Constructed Sandwich-Like Nanosheets as Bifunctional Catalysts for Direct Formic Acid Fuel Cells.* ACS Applied Energy Materials, 2021. **4**(11): p. 12336-12344.

20.   Li, Y., et al., *Catalyst Electrodes with PtCu Nanowire Arrays In Situ Grown on Gas Diffusion Layers for Direct Formic Acid Fuel Cells.* ACS applied materials & interfaces, 2022. **14**(9): p. 11457-11464.

21.   Dutta, I., et al., *Formic Acid to Power towards Low-Carbon Economy.* Advanced Energy Materials, 2022. **12**(15): p. 2103799.

22.   da Silva Cardoso, R., et al., *Pt Electrocatalyst Prepared by Hydrothermal Reduction onto the Gas Diffusion Layer for High-Temperature Formic Acid and Ethanol Fuel PEMFC.* Catalysts, 2021. **11**(10): p. 1246.

23.   Williams, R., R.S. Crandall, and A. Bloom, *Use of carbon dioxide in energy storage.* Applied Physics Letters, 1978. **33**(5): p. 381-383.

24.   Sordakis, K., et al., *Homogeneous catalysis for sustainable hydrogen storage in formic acid and alcohols.* Chemical reviews, 2018. **118**(2): p. 372-433.

25.   Bulushev, D.A., S. Beloshapkin, and J.R. Ross, *Hydrogen from formic acid decomposition over Pd and Au catalysts.* Catalysis today, 2010. **154**(1-2): p. 7-12.

26.   Hu, C., et al., *Reaction pathways derived from DFT for understanding catalytic decomposition of formic acid into hydrogen on noble metals.* International journal of hydrogen energy, 2012. **37**(21): p. 15956-15965.

27.   Yuranov, I., et al., *Heterogeneous catalytic reactor for hydrogen production from formic acid and its use in polymer electrolyte fuel cells.* ACS Sustainable Chemistry & Engineering, 2018. **6**(5): p. 6635-6643.

28.   Laurenczy, G. and P.J. Dyson, *Homogeneous catalytic dehydrogenation of formic acid: progress towards a hydrogen-based economy.* Journal of the Brazilian Chemical Society, 2014. **25**: p. 2157-2163.

29.   Schaub, T. and R.A. Paciello, *A process for the synthesis of formic acid by CO2 hydrogenation: thermodynamic aspects and the role of CO.* Angewandte Chemie International Edition, 2011. **50**(32): p. 7278-7282.

30. Sanni, S.E., et al., *Strategic examination of the classical catalysis of formic acid decomposition for intermittent hydrogen production, storage and supply: A review.* Sustainable Energy Technologies and Assessments, 2021. **45**: p. 101078.

31. Johnson, T.C., D.J. Morris, and M. Wills, *Hydrogen generation from formic acid and alcohols using homogeneous catalysts.* Chemical Society Reviews, 2010. **39**(1): p. 81-88.

32. Bulushev, D.A. and J.R. Ross, *Towards sustainable production of formic acid.* ChemSusChem, 2018. **11**(5): p. 821-836.

33. Zhang, L., et al., *A review on liquid-phase heterogeneous dehydrogenation of formic acid: Recent advances and perspectives.* Chemical Papers, 2018. **72**(9): p. 2121-2135.

34. Lanz, A., J. Heffel, and C. Messer, *Hydrogen fuel cell engines and related technologies*. 2001, United States. Department of Transportation. Federal Transit Administration.

35. Hassan, I., et al., *Hydrogen storage technologies for stationary and mobile applications: Review, analysis and perspectives.* Renewable and Sustainable Energy Reviews, 2021. **149**: p. 111311.

36. Andersson, J. and S. Grönkvist, *Large-scale storage of hydrogen.* International journal of hydrogen energy, 2019. **44**(23): p. 11901-11919.

37. Yadav, M. and Q. Xu, *Liquid-phase chemical hydrogen storage materials.* Energy & Environmental Science, 2012. **5**(12): p. 9698-9725.

38. El-Shafie, M., S. Kambara, and Y. Hayakawa, *Hydrogen production technologies overview.* 2019.

39. Kalamaras, C.M. and A.M. Efstathiou, *Hydrogen production technologies: current state and future developments. Conference papers in energy 2013.* Article ID, 2013. **690627**(9).

40. Kannah, R. and S. Kavitha, *Preethi; Karthikeyan, OP; Kumar, G.; Dai-Viet, NV; Rajesh Banu, J.* Techno-economic assessment of various hydrogen production methods–A review. Bioresour. Technol, 2021. **319**: p. 124175.

41. Nikolaidis, P. and A. Poullikkas, *A comparative overview of hydrogen production processes.* Renewable and sustainable energy reviews, 2017. **67**: p. 597-611.

42. Dang, T.N.M., et al., *Effect of impurities on glycerol steam reforming over Ni-promoted metallurgical waste driven catalyst.* International Journal of Hydrogen Energy, 2022. **47**(7): p. 4614-4630.

43. Sahraei, O.A., et al., *Ni-Fe catalyst derived from mixed oxides Fe/Mg-bearing metallurgical waste for hydrogen production by steam reforming of biodiesel by-product: Investigation of catalyst synthesis parameters and temperature dependency of the reaction network.* Applied Catalysis B: Environmental, 2020. **279**: p. 119330.

44. Charisiou, N., et al., *An in depth investigation of deactivation through carbon formation during the biogas dry reforming reaction for Ni supported on modified with CeO2 and La2O3 zirconia catalysts.* International Journal of Hydrogen Energy, 2018. **43**(41): p. 18955-18976.

45. Hajizadeh, A., et al., *Hydrogen production from biomass through integration of anaerobic digestion and biogas dry reforming.* Applied Energy, 2022. **309**: p. 118442.

46. Yoo, S., et al., *Hydrogen production by the steam reforming of ethanol over K-promoted Co/Al2O3–CaO xerogel catalysts.* Molecular Catalysis, 2020. **491**: p. 110980.

47.   Pafili, A., et al., *Recent Progress in the Steam Reforming of Bio-Oil for Hydrogen Production: A Review of Operating Parameters, Catalytic Systems and Technological Innovations.* Catalysts, 2021. **11**(12): p. 1526.

48.   Megía, P., et al., *Coke evolution in simulated bio-oil aqueous fraction steam reforming using Co/SBA-15.* Catalysis Today, 2021. **367**: p. 145-152.

49.   Shahbaz, M., et al., *A state of the art review on biomass processing and conversion technologies to produce hydrogen and its recovery via membrane separation.* International Journal of Hydrogen Energy, 2020. **45**(30): p. 15166-15195.

50.   Azwar, M., M. Hussain, and A. Abdul-Wahab, *Development of biohydrogen production by photobiological, fermentation and electrochemical processes: a review.* Renewable and Sustainable Energy Reviews, 2014. **31**: p. 158-173.

51.   Hosseini, S.E., et al., *A review on biomass-based hydrogen production for renewable energy supply.* International journal of energy research, 2015. **39**(12): p. 1597-1615.

52.   Sivaramakrishnan, R., et al., *Insights on biological hydrogen production routes and potential microorganisms for high hydrogen yield.* Fuel, 2021. **291**: p. 120136.

53.   Das, D. and T.N. Veziroğlu, *Hydrogen production by biological processes: a survey of literature.* International journal of hydrogen energy, 2001. **26**(1): p. 13-28.

54.   Akhlaghi, N. and G. Najafpour-Darzi, *A comprehensive review on biological hydrogen production.* International Journal of Hydrogen Energy, 2020. **45**(43): p. 22492-22512.

55.   Kumar, G., et al., *Biomass based hydrogen production by dark fermentation—recent trends and opportunities for greener processes.* Current Opinion in Biotechnology, 2018. **50**: p. 136-145.

56.   Ghimire, A., et al., *A review on dark fermentative biohydrogen production from organic biomass: process parameters and use of by-products.* Applied Energy, 2015. **144**: p. 73-95.

57.   Hitam, C. and A. Jalil, *A review on biohydrogen production through photo-fermentation of lignocellulosic biomass.* Biomass Conversion and Biorefinery, 2020: p. 1-19.

58.   Arregi, A., et al., *Evaluation of thermochemical routes for hydrogen production from biomass: A review.* Energy conversion and management, 2018. **165**: p. 696-719.

59.   Gemechu, E.D., et al., *Life Cycle Assessment of the Environmental Performance of Thermochemical Processing of Biomass.* Thermochemical Processing of Biomass: Conversion into Fuels, Chemicals and Power, 2019: p. 355-378.

60.   Lepage, T., et al., *Biomass-to-hydrogen: A review of main routes production, processes evaluation and techno-economical assessment.* Biomass and Bioenergy, 2021. **144**: p. 105920.

61.   Pandey, B., Y.K. Prajapati, and P.N. Sheth, *Recent progress in thermochemical techniques to produce hydrogen gas from biomass: A state of the art review.* International Journal of Hydrogen Energy, 2019. **44**(47): p. 25384-25415.

62.   Tanksale, A., J.N. Beltramini, and G.M. Lu, *A review of catalytic hydrogen production processes from biomass.* Renewable and Sustainable Energy Reviews, 2010. **14**(1): p. 166-182.

63.   Shayan, E., V. Zare, and I. Mirzaee, *Hydrogen production from biomass gasification; a theoretical comparison of using different gasification agents.* Energy Conversion and management, 2018. **159**: p. 30-41.

64. Rapagnà, S., N. Jand, and P. Foscolo, *Catalytic gasification of biomass to produce hydrogen rich gas.* International journal of hydrogen energy, 1998. **23**(7): p. 551-557.

65. Xie, Q., et al., *Syngas production by two-stage method of biomass catalytic pyrolysis and gasification.* Bioresource technology, 2012. **110**: p. 603-609.

66. Yung, M.M., et al., *Biomass catalytic pyrolysis on Ni/ZSM-5: effects of nickel pretreatment and loading.* Energy & Fuels, 2016. **30**(7): p. 5259-5268.

67. Cho, S.-H., et al., *Synergistic effects of CO2 on ex situ catalytic pyrolysis of lignocellulosic biomass over a Ni/SiO2 catalyst.* Journal of CO2 Utilization, 2020. **39**: p. 101182.

68. Dai, L., et al., *A review on selective production of value-added chemicals via catalytic pyrolysis of lignocellulosic biomass.* Science of the Total Environment, 2020. **749**: p. 142386.

69. Chireshe, F., F.-X. Collard, and J.F. Görgens, *Production of an upgraded bio-oil with minimal water content by catalytic pyrolysis: Optimisation and comparison of CaO and MgO performances.* Journal of Analytical and Applied Pyrolysis, 2020. **146**: p. 104751.

70. Ma, C., et al., *Non-catalytic and catalytic pyrolysis of Ulva prolifera macroalgae for production of quality bio-oil.* Journal of the Energy Institute, 2020. **93**(1): p. 303-311.

71. Chi, J. and H. Yu, *Water electrolysis based on renewable energy for hydrogen production.* Chinese Journal of Catalysis, 2018. **39**(3): p. 390-394.

72. Kumar, S.S. and V. Himabindu, *Hydrogen production by PEM water electrolysis–A review.* Materials Science for Energy Technologies, 2019. **2**(3): p. 442-454.

73. Alfredo, U., M. Gandia Luis, and S. Pablo, *Hydrogen production from water electrolysis: current status and future trends.* Proc. IEEE, 2012. **100**: p. 410-426.

74. Feng, Q., et al., *A review of proton exchange membrane water electrolysis on degradation mechanisms and mitigation strategies.* Journal of Power Sources, 2017. **366**: p. 33-55.

75. Holladay, J.D., et al., *An overview of hydrogen production technologies.* Catalysis today, 2009. **139**(4): p. 244-260.

76. Jafari, T., et al., *Photocatalytic water splitting—the untamed dream: a review of recent advances.* Molecules, 2016. **21**(7): p. 900.

77. Eidsvåg, H., et al., *TiO2 as a photocatalyst for water splitting—An experimental and theoretical review.* Molecules, 2021. **26**(6): p. 1687.

78. Park, Y.-K., et al., *Characteristics of hydrogen production by photocatalytic water splitting using liquid phase plasma over Ag-doped TiO2 photocatalysts.* Environmental Research, 2020. **188**: p. 109630.

79. Liu, L., et al., *Water-Stable Nickel Metal–Organic Framework Nanobelts for Cocatalyst-Free Photocatalytic Water Splitting to Produce Hydrogen.* Journal of the American Chemical Society, 2022. **144**(6): p. 2747-2754.

80. Bulushev, D.A., *Progress in catalytic hydrogen production from formic acid over supported metal complexes.* Energies, 2021. **14**(5): p. 1334.

81. Bulushev, D.A. and L.G. Bulusheva, *Catalysts with single metal atoms for the hydrogen production from formic acid.* Catalysis Reviews, 2021: p. 1-40.

82.   Bulushev, D.A., et al., *Ni-N4 sites in a single-atom Ni catalyst on N-doped carbon for hydrogen production from formic acid.* Journal of Catalysis, 2021. **402**: p. 264-274.

83.   Carrales-Alvarado, D., et al., *Effect of N-doping and carbon nanostructures on NiCu particles for hydrogen production from formic acid.* Applied Catalysis B: Environmental, 2021. **298**: p. 120604.

84.   Liu, T., et al., *Pd nanoparticles immobilized on aniline-functionalized MXene as an effective catalyst for hydrogen production from formic acid.* International Journal of Hydrogen Energy, 2021. **46**(66): p. 33098-33106.

85.   Santos, J.L., et al., *Functionalized biochars as supports for Pd/C catalysts for efficient hydrogen production from formic acid.* Applied Catalysis B: Environmental, 2021. **282**: p. 119615.

86.   Cai, L., et al., *Pt-based intermetallic compounds with tunable activity and selectivity toward hydrogen production from formic acid.* Applied Surface Science, 2022. **597**: p. 153530.

87.   Shaybanizadeh, S., A.N. Chermahini, and R. Luque, *Boron nitride nanosheets supported highly homogeneous bimetallic AuPd alloy nanoparticles catalyst for hydrogen production from formic acid.* Nanotechnology, 2022. **33**(27): p. 275601.

88.   Xu, J., et al., *Nitrogen/oxygen co-doped graphene bonded nickel particles composite for dehydrogenation of formic acid at near room temperature.* International Journal of Hydrogen Energy, 2022. **47**(3): p. 1765-1774.

89.   Zhang, M., et al., *In-situ Derived MOF@ In2S3 Heterojunction Stabilizes Co (II)-Salicylaldimine for Efficient Photocatalytic Formic Acid Dehydrogenation.* Chemical Communications, 2022.

90.   Nouruzi, N., et al., *Photocatalytic hydrogen generation using colloidal covalent organic polymers decorated bimetallic Au-Pd nanoalloy (COPs/Pd-Au).* Molecular Catalysis, 2022. **518**: p. 112058.

91.   Zhang, S., et al., *MoS2/Zn3In2S6 composite photocatalysts for enhancement of visible light-driven hydrogen production from formic acid.* Chinese Journal of Catalysis, 2021. **42**(1): p. 193-204.

92.   Ibarra-Rodriguez, L.I., et al., *Formic acid and hydrogen generation from the photocatalytic reduction of CO2 on visible light activated N-TiO2/CeO2/CuO composites.* Journal of Photochemistry and Photobiology, 2022. **11**: p. 100125.

93.   Suhag, M.H., et al., *Photocatalytic Hydrogen Production from Formic Acid Solution with Titanium Dioxide with the Aid of Simultaneous Rh Deposition.* ChemEngineering, 2022. **6**(3): p. 43.

94.   Gao, Y., et al., *The interconversion of formic acid and hydrogen/carbon dioxide using a binuclear ruthenium complex catalyst.* Journal of the Chemical Society, Dalton Transactions, 2000(18): p. 3212-3217.

95.   Patra, S. and S.K. Singh, *Hydrogen production from formic acid and formaldehyde over ruthenium catalysts in water.* Inorganic Chemistry, 2020. **59**(7): p. 4234-4243.

96.   Boddien, A., et al., *Continuous hydrogen generation from formic acid: highly active and stable ruthenium catalysts.* Advanced Synthesis & Catalysis, 2009. **351**(14-15): p. 2517-2520.

97.   Gan, W., P.J. Dyson, and G. Laurenczy, *Hydrogen storage and delivery: immobilization of a highly active homogeneous catalyst for the decomposition of formic acid to hydrogen and carbon dioxide.* Reaction Kinetics and Catalysis Letters, 2009. **98**(2): p. 205-213.

98.   Barnard, J.H., et al., *Long-range metal–ligand bifunctional catalysis: cyclometallated iridium catalysts for the mild and rapid dehydrogenation of formic acid.* Chemical Science, 2013. **4**(3): p. 1234-1244.

99.   Guo, J., et al., *Picolinamide-Based Iridium Catalysts for Aqueous Formic Acid Dehydrogenation: Increase in Electron Density of Amide N through Substituents.* Asian Journal of Organic Chemistry, 2022. **11**(1): p. e202100562.

100.   Navlani-García, M., et al., *New approaches toward the hydrogen production from formic acid dehydrogenation over Pd-based heterogeneous catalysts.* Frontiers in Materials, 2019. **6**: p. 44.

101.   Li, J., Q.-L. Zhu, and Q. Xu, *Dehydrogenation of formic acid by heterogeneous catalysts.* Chimia, 2015. **69**(6): p. 348-348.

102.   Hu, C., et al., *Activity of Pd/C for hydrogen generation in aqueous formic acid solution.* International journal of hydrogen energy, 2014. **39**(1): p. 381-390.

103.   Bulushev, D.A., et al., *Hydrogen production from formic acid over au catalysts supported on carbon: Comparison with Au catalysts supported on SiO2 and Al2O3.* Catalysts, 2019. **9**(4): p. 376.

104.   Chesnokov, V., et al., *Decomposition of Formic Acid on Pt/N-Graphene.* Kinetics and Catalysis, 2021. **62**(4): p. 518-527.

105.   Faroldi, B., et al., *Efficient nickel and copper-based catalysts supported on modified graphite materials for the hydrogen production from formic acid decomposition.* Applied Catalysis A: General, 2022. **629**: p. 118419.

106.   Zhang, S.-L., et al., *Amine-functionalized carbon nanotubes supported NiAuPd nanoparticles as an efficient in-situ prepared catalyst for formic acid dehydrogenation.* International Journal of Hydrogen Energy, 2021. **46**(70): p. 34727-34736.

107.   Yang, Y., et al., *Hydrogen production via efficient formic acid decomposition: engineering the surface structure of Pd-based alloy catalysts by design.* ACS Catalysis, 2018. **9**(1): p. 781-790.

108.   Sun, J., et al., *Ultrafine Pd particles embedded in nitrogen-enriched mesoporous carbon for efficient H2 production from formic acid decomposition.* ACS Sustainable Chemistry & Engineering, 2018. **7**(2): p. 1963-1972.

109.   Sneka-Płatek, O., et al., *Understanding the influence of the composition of the AgPd catalysts on the selective formic acid decomposition and subsequent levulinic acid hydrogenation.* International Journal of Hydrogen Energy, 2020. **45**(35): p. 17339-17353.

110.   Santos, J.L., et al., *Structure-sensitivity of formic acid dehydrogenation reaction over additive-free Pd NPs supported on activated carbon.* Chemical Engineering Journal, 2021. **420**: p. 127641.

111.   Qiu, H., et al., *Effect of different doping ratios of Cu on the carbon formation and the elimination on Ni (111) surface: A DFT study.* Molecular Catalysis, 2021. **502**: p. 111360.

112.   Guo, X., et al., *Carbon formation and steam reforming of methane on silica supported nickel catalysts.* Catalysis Communications, 2012. **19**: p. 61-65.

113.   Charisiou, N.D., et al., *The relationship between reaction temperature and carbon deposition on nickel catalysts based on Al2O3, ZrO2 or SiO2 supports during the biogas dry reforming reaction.* Catalysts, 2019. **9**(8): p. 676.

114. Graschinsky, C., et al., *Thermodynamic analysis of hydrogen production by autothermal reforming of ethanol.* International journal of hydrogen energy, 2012. **37**(13): p. 10118-10124.

115. Kihlman, J., et al., *Whisker carbon formation in catalytic steam reforming of biomass gasification gas.* Applied Catalysis A: General, 2018. **564**: p. 133-141.

116. Kihlman, J. and P. Simell, *Carbon Formation in the Reforming of Simulated Biomass Gasification Gas on Nickel and Rhodium Catalysts.* Catalysts, 2022. **12**(4): p. 410.

117. Hu, X., et al., *Coke formation during thermal treatment of bio-oil.* Energy & Fuels, 2020. **34**(7): p. 7863-7914.

118. Li, Y., et al., *Coke formation on the surface of Ni/HZSM-5 and Ni-Cu/HZSM-5 catalysts during bio-oil hydrodeoxygenation.* Fuel, 2017. **189**: p. 23-31.

119. Li, X., et al., *A mechanistic study on the decomposition of a model bio-oil compound for hydrogen production over a stepped Ni surface: Formic acid.* Applied Surface Science, 2018. **452**: p. 87-95.

120. Hafeez, S., et al., *Decomposition of additive-free formic acid using a pd/c catalyst in flow: Experimental and cfd modelling studies.* Catalysts, 2021. **11**(3): p. 341.

121. Sanchez, F., et al., *Hydrogen generation from additive-free formic acid decomposition under mild conditions by Pd/C: Experimental and DFT studies.* Topics in catalysis, 2018. **61**(3): p. 254-266.

122. Stegehake, C., J. Riese, and M. Grünewald, *Modeling and Validating Fixed-Bed Reactors: A State-of-the-Art Review.* ChemBioEng Reviews, 2019. **6**(2): p. 28-44.

123. Jurtz, N., M. Kraume, and G.D. Wehinger, *Advances in fixed-bed reactor modeling using particle-resolved computational fluid dynamics (CFD).* Reviews in Chemical Engineering, 2019. **35**(2): p. 139-190.

124. Nienow, A.W., *Stirring and stirred-tank reactors.* Chemie Ingenieur Technik, 2014. **86**(12): p. 2063-2074.

125. Simorgh, A., A. Razminia, and V.I. Shiryaev, *System identification and control design of a nonlinear continuously stirred tank reactor.* Mathematics and Computers in Simulation, 2020. **173**: p. 16-31.

126. Froment, G.F., K.B. Bischoff, and J. De Wilde, *Chemical reactor analysis and design*. Vol. 2. 1990: Wiley New York.

127. Dupont, N., et al., *Specificities of micro-structured reactors for hydrogen production and purification.* International journal of hydrogen energy, 2007. **32**(10-11): p. 1443-1449.

128. Solymosi, F., et al., *Production of CO-free H2 from formic acid. A comparative study of the catalytic behavior of Pt metals on a carbon support.* Journal of catalysis, 2011. **279**(1): p. 213-219.

129. Koós, Á. and F. Solymosi, *Production of CO-free H2 by formic acid decomposition over Mo2C/carbon catalysts.* Catalysis letters, 2010. **138**(1): p. 23-27.

130. Winkler, T., et al., *Catalytic decomposition of formic acid in a fixed bed reactor–an experimental and modelling study.* Catalysis Today, 2022. **387**: p. 128-139.

131. Zhu, S., et al., *Low Temperature H 2 Production from Formic Acid Aqueous Solution Catalyzed on Metal Doped Mo 2 C.* Journal of Renewable Materials, 2020. **8**(8): p. 939.

132. Faroldi, B., et al., *Hydrogen Production by Formic Acid Decomposition over Ca Promoted Ni/SiO2 Catalysts: Effect of the Calcium Content.* Nanomaterials, 2019. **9**(11): p. 1516.

133. Bulushev, D.A., et al., *Catalytic properties of PdZn/ZnO in formic acid decomposition for hydrogen production.* Applied Catalysis A: General, 2018. **561**: p. 96-103.

134. Sobolev, V., I. Asanov, and K. Koltunov, *The role of support in formic acid decomposition on gold catalysts.* Energies, 2019. **12**(21): p. 4198.

135. Hafeez, S., et al., *Experimental and Process Modelling Investigation of the Hydrogen Generation from Formic Acid Decomposition Using a Pd/Zn Catalyst.* Applied Sciences, 2021. **11**(18): p. 8462.

136. Xu, P., F.D. Bernal-Juan, and L. Lefferts, *Effect of oxygen on formic acid decomposition over Pd catalyst.* Journal of catalysis, 2021. **394**: p. 342-352.

137. Ellwood, T., et al., *Process intensification in photocatalytic decomposition of formic acid over a tio2 catalyst by forced periodic modulation of concentration, temperature, flowrate and light intensity.* Processes, 2021. **9**(11): p. 2046.

138. Caiti, M., D. Padovan, and C. Hammond, *Continuous production of hydrogen from formic acid decomposition over heterogeneous nanoparticle catalysts: From batch to continuous flow.* ACS Catalysis, 2019. **9**(10): p. 9188-9198.

139. Ndlovu, I.M., et al., *A performance evaluation of a microchannel reactor for the production of hydrogen from formic acid for electrochemical energy applications.* 2017.

140. Wang, J., et al., *Non-precious molybdenum-based catalyst derived from biomass: CO-free hydrogen production from formic acid at low temperature.* Energy Conversion and Management, 2018. **164**: p. 122-131.

141. Wang, J., et al., *Decomposition of formic acid for hydrogen production over metal doped nanosheet-like MoC1– x catalysts.* Energy Conversion and Management, 2017. **147**: p. 166-173.

142. Hafeez, S., et al., *Computational Investigation of Microreactor Configurations for Hydrogen Production from Formic Acid Decomposition Using a Pd/C Catalyst.* Industrial & Engineering Chemistry Research, 2022.

143. Hu, C., et al., *Formic acid dehydrogenation over PtRuBiOx/C catalyst for generation of CO-free hydrogen in a continuous-flow reactor.* International journal of hydrogen energy, 2012. **37**(8): p. 6372-6380.

144. Zhao, Z., et al., *Hydrogen-generating behavior of Pd-decorated gold nanoparticles via formic acid decomposition.* Catalysis Today, 2019. **330**: p. 24-31.

145. Sun, X., A. Constantinou, and A. Gavriilidis, *Stripping of acetone from isopropanol solution with membrane and mesh gas–liquid contactors.* Chemical Engineering and Processing: Process Intensification, 2011. **50**(10): p. 991-997.

146. Guettel, R. and T. Turek, *Assessment of micro-structured fixed-bed reactors for highly exothermic gas-phase reactions.* Chemical Engineering Science, 2010. **65**(5): p. 1644-1654.